

Accepted Manuscript

Graphene-philic surfactants for nanocomposites in latex technology

Azmi Mohamed, Tretya Ardyani, Suriani Abu Bakar, Paul Brown, Martin Hollamby, Masanobu Sagisaka, Julian Eastoe

PII: S0001-8686(16)30014-8
DOI: doi: [10.1016/j.cis.2016.01.003](https://doi.org/10.1016/j.cis.2016.01.003)
Reference: CIS 1616

To appear in: *Advances in Colloid and Interface Science*



Please cite this article as: Mohamed Azmi, Ardyani Tretya, Bakar Suriani Abu, Brown Paul, Hollamby Martin, Sagisaka Masanobu, Eastoe Julian, Graphene-philic surfactants for nanocomposites in latex technology, *Advances in Colloid and Interface Science* (2016), doi: [10.1016/j.cis.2016.01.003](https://doi.org/10.1016/j.cis.2016.01.003)

This is a PDF file of an unedited manuscript that has been accepted for publication. As a service to our customers we are providing this early version of the manuscript. The manuscript will undergo copyediting, typesetting, and review of the resulting proof before it is published in its final form. Please note that during the production process errors may be discovered which could affect the content, and all legal disclaimers that apply to the journal pertain.

Graphene-philic surfactants for nanocomposites in latex technology

Azmi Mohamed^{1,2*}, Tretya Ardyani¹, Suriani Abu Bakar² Paul Brown³, Martin Hollamby⁴,
Masanobu Sagisaka⁵, Julian Eastoe⁶

¹Department of Chemistry, Faculty of Science and Mathematics, Universiti Pendidikan Sultan Idris, 35900 Tanjong Malim, Perak, Malaysia

²Nanotechnology Research Centre, Faculty of Science and Mathematics, Universiti Pendidikan Sultan Idris, 35900 Tanjong Malim, Perak, Malaysia

³Department of Chemical Engineering, Massachusetts Institute of Technology, 77 Massachusetts Avenue, Cambridge, Massachusetts 02139, United States

⁴School of Physical and Geographical Sciences, Keele University, Staffordshire ST5 5BG United Kingdom

⁵Department of Frontier Materials Chemistry, Graduate School of Science and Technology, Hirosaki University, Bunkyo-cho 3, Hirosaki, Aomori 036-8561, Japan

⁶School of Chemistry, University of Bristol, Cantock's Close, Bristol, BS8 1TS, United Kingdom

*Corresponding author. Tel.: +601548117582; fax: +601548117296

E-mail address: azmi.mohamed@fsmt.upsi.edu.my

Abstract

Graphene is the newest member of the carbon family, and has revolutionized materials science especially in the field of polymer nanocomposites. However, agglomeration and uniform dispersion remains an Achilles' heel (even an elephant in the room), hampering the optimization of this material for practical applications. Chemical functionalization of graphene can overcome these hurdles but is often rather disruptive to the extended pi-conjugation, altering the desired physical and electronic properties. Employing surfactants as stabilizing agents in latex technology circumvents the need for chemical modification allowing for the formation of nanocomposites with retained graphene properties. This article reviews the recent progress in the use of surfactants and polymers to prepare graphene/polymer nanocomposites via latex technology. Of special interest here are surfactant structure-performance relationships, as well as background on the roles surfactant-graphene interactions for promoting stabilization.

Keywords: graphene, nanocomposites, surfactants, stabilization, latex technology

Contents of Paper

1. Introduction
 - 1.1 Why graphene?
 - 1.2 Graphene-polymer nanocomposites: Challenges and prospects
 - 1.3 Surfactant and latex technology
2. Graphene-compatible surfactants
 - 2.1 Ionic surfactants
 - 2.2 Nonionic surfactants
 - 2.3 Polymeric surfactants
3. Specific applications of surfactant
 - 3.1 Surfactant stabilization: The DLVO theory and steric forces
 - 3.2 Dispersion mechanism: surfactant-graphene interactions
 - 3.3 Simulation of surfactant self-assembly on graphene surfaces
4. Polymers
 - 4.1 Hydrocarbon polymers
 - 4.2 Oxygenated polymers
5. Applications and industrial relevance
6. Conclusions

1. Introduction

1.1 Why graphene?

Graphene research fills the pages of scientific journals and is, without doubt, the “material du jour” in many disciplines [1]. Since its discovery in 2004 [2, 3], it has been impossible to ignore the enormous experimental and theoretical efforts that have been devoted to unveiling its fascinating physical and mechanical properties [4-12]. Strictly speaking, graphene is a two dimensional (2D) sheet of sp^2 conjugated carbon atoms arrayed in a honeycomb lattice [1, 13]. It is widely viewed as the building block for other allotropes of carbon such as fullerenes (0D), graphite (3D) and carbon nanotubes (CNTs, 1D) [14]. Properties such as high mechanical strength [15], large surface area [16], excellent thermal [17] and electrical conductivity [18] and its quasi-transparency, absorbing only 2.3% of incident white light [19] have led graphene to be implemented in a myriad of devices (at least in academic literature) such as sensors, transparent electrodes, thin films and composite materials [17, 20-23].

However, despite much hyperbole, there are still many challenges which need to be addressed before graphene can appear on the market. Such factors include cost and limited production volume. All current methods are unable to reliably produce high quality gram-scale quantities of graphene without defects or impurities. For example, attempts to mechanically exfoliate graphite using the “Scotch-tape” method is laborious and has only ever resulted in a few isolated sheets in low yields [3]. Alternatives to mechanical exfoliation, such as the epitaxial growth method, can produce high-quality graphene, but it requires expensive systems and high-vacuum not accessible in all research laboratories [24]. To-date, the reduction of graphene derivatives, such as graphene oxide, stands out as a suitable strategy to yield bulk amounts of graphene, albeit not completely defect-free and sometimes involving pricey or toxic chemicals [25, 26]. Reduced graphene oxide (rGO) also suffers

from irreversible aggregation due to the loss of oxygen-containing functional groups during the chemical reduction process.

1.2 Graphene-polymer nanocomposites: Challenges and opportunities

The impressive popularity of graphene inevitably attracted researchers from the field of polymer nanocomposites [27-30]. Until very recently, research into polymer nanocomposites focused mainly on carbon nanotubes (CNTs) [31-33]. Now, graphene is predicted to supplant CNT as the filler of choice for polymer reinforcement [34-37] and is promising to revolutionize the use of traditional polymeric reinforcing agents such as carbon black [38, 39] and silica [40, 41]. The first mention of graphene as a nanofiller was reported by Stankovich and co-workers [17]. They demonstrated the ability of graphene to provide multifunctional enhancement at a relatively small loading; around 0.1 - 2 vol% [17, 29, 42]. When dispersed in a polymer matrix, graphene can provide properties which are conventionally only achieved by using a combination of two or more fillers, such as silicates (gas permeation barrier) and CNTs (thermal and electrical conductivity) [38, 43-46].

To produce nanocomposites of this kind is not without limitations. One major barrier to using graphene for polymeric reinforcement is that it has very low solubility (insoluble) in most solvents [47-50]. Moreover, in order to harness the inherent properties of graphene the material should be finely dispersed in the polymer host, requiring intensified interfacial interactions between the polymer chains and graphene surface [17]. However, to obtain a uniform dispersion of graphene in polymer matrices is quite challenging since the material tends to self-associate into micro-scale aggregates (bundles in the case of CNTs) or stacked into more graphitic layered structures due to the strong van der Waals interactions between graphene sheets [47, 49, 51]. In this way, it is nearly impossible to achieve the optimum reinforcement with polymer reinforced individual graphene.

Various methods have been developed to incorporate graphene into polymer matrices including solution mixing, melt blending and in-situ polymerization. Alas, each method has its drawbacks and restacking of the graphene sheets persistently occurs [31, 52, 53]. In order to provide a good dispersion of graphene in polymer matrices, the destabilizing van der Waals interactions should be overcome, without perturbing the graphene sheets. Two common methods to improve the dispersion quality of graphene are through the alteration of the graphene surfaces either via covalent or non-covalent modifications. Covalent approaches through functionalization can significantly enhance the interaction of “inert” graphene with polymer matrices. However, the presence of functional groups introduces defects and disrupts the extended sp^2 conjugated network, thus limiting the reinforcing enhancement [54-56]. Meanwhile non-covalent approaches are based on weak intermolecular interactions e.g. π - π stacking, van der Waals forces and electrostatic interactions with graphene surfaces, or they rely on the stabilization effects of a third added component, such as polymers or surfactants [57-59]. This approach is particularly attractive because it offers improvements in graphene dispersion on the one hand, while minimizing the loss of desired properties on the other [59, 60]. In some cases though, the presence of stabilizers may affect the mechanical properties of the final graphene loaded products [27, 61, 62], as also observed with CNTs [63]. Because amphiphilic surfactant molecules have proven particularly useful in achieving stable graphene suspensions, they are the focus of interest throughout this review.

1.3 Surfactant and latex technology

Latex technology now employs surfactants to assist in the incorporation of graphene into polymer matrices. The principle was introduced back in the 1980's when used to modify the dispersibility of clay minerals in a polymer matrices. The idea was put forth by Lagaly and others to make polymer reinforced clay nanocomposites [64]. When dispersed into polymer matrices, it is difficult to design exfoliated clay-polymer nanocomposites because of the tendency to agglomerate into tactoids, rather than forming discrete monolayers. Complete (or nearly so) exfoliation, can be achieved by the use of surfactants or organic compounds. Many articles have been written on this topic, and interested readers are referred elsewhere for details [65-67]. One breakthrough in materials science came from the discovery of carbon nanotubes by Sumio Ijima in 1991. The material has had a meteoric rise since then, and parallel efforts mostly on conductive nanocomposites have provided the major thrust of investigations. Latex technology was again employed to achieve compatibility between surfactants and CNTs for aqueous based dispersions [68-70]. However, there is no generally accepted definition of the term "latex technology". Some confusion about the meaning of this term has ensued with surfactant-free systems also being considered [29, 71-73]. To avoid arbitrary distinctions with other latex-based methods [29, 53, 71], the term "latex technology" will be applied throughout this study to refer the fabrication of composites with colloidal systems, comprising aqueous dispersions of nanofillers and polymer matrices stabilized by surfactants which bind non-covalently to the filler surfaces. The processes are simple and typically consist of mixing aqueous surfactant-filler dispersions by means of ultrasonication followed by dispersion with the polymer matrix of choice.

The preparation of graphene/polymer nanocomposites via latex technology (see Fig.1.) was pioneered by Tkalya et al. [27]. The group revealed that graphene/polymer

nanocomposites prepared in this way exhibited relatively good dispersion quality, and thus gave a pronounced enhancement of properties e.g. electrical conductivity as compared to those prepared using other techniques. The electrical and thermal properties of carbon nanomaterial/polymer composites are widely described using percolation theory, though the term “thermal percolation” is still a subject of debate [74, 75]. In the case of electrical percolation, at very low filler loadings, the conductivities remain very close to the insulating pure polymers since the fillers are in a random arrangement. At a certain graphene concentration i.e. percolation threshold, the conductivity increases sharply (by several orders of magnitude), after which there is no significant change in the electrical properties of the composites. This change corresponds to the formation of a filler network within the matrix for enhanced electron mobility [17, 76]. The versatility of latex technology to offer low percolation threshold and relatively high conductivity immediately stimulated others to work in this area, with much success [27, 38, 44, 61]. Also spurred on by the desire to minimize the use of organic solvents, so-called volatile organic compounds (VOCs). The avoidance of VOCs in material processing is a positive step towards the more environmentally friendly handling of graphene. With these factors in mind, nanocomposite production using this technique is expected to pave the way for further research and development.

To achieve graphene dispersibility for latex technology processing, surfactants which are active at the graphene surface are needed. The unique features of surfactants for changing surface energy and aggregation to form micelles are important to facilitate the formation of stable colloidal systems. At the graphene-solution interface, the surfactant tails are adsorbed – driven by hydrophobic interactions helping to separate the graphene sheets to prevent agglomeration via electrostatic or steric stabilization [60, 77]. Unfortunately, relatively few commercial surfactants exhibit any significant compatibility with graphene, and the systematic design of graphene-compatible surfactants is only in its infancy.

Moreover, the presence of surfactants in the polymer films, and an understanding of their effects on nanocomposite properties are still lacking in the literature. Studies have reported that surfactants can mediate filler-polymer interactions and enhance the filler-to-matrix transfer properties [42, 44, 69, 70, 78], though different conclusions were reached. Juhué et al. [79, 80] noted that the properties of the resulting polymer films are influenced by the nature of the polymer, particle size and distribution, particle morphology and the amount of surfactant. With regard to nanofiller properties, Zuberi et al. [81] and Lisunova et al. [82] both presumed that the presence of a surfactant insulating layer atop the nanofiller surface would hinder the electron mobility between the nanofiller conductive network to give higher resistivity values. Recently, Tkalya et al. [27] also showed this, by using high surfactant levels (up to 10-fold excess) to obtain stable graphene dispersions. The presence of excess surfactant in the final composites was acknowledged to affect the ability of graphene to fully enhance the electrical conductivity of the resulting nanocomposites. Therefore, there is an imperative to search for new types of surfactant which can efficiently provide a good dispersion quality at low loading.

Interestingly, surfactant stabilization in graphene/polymer matrices occurs in a similar manner to CNT/surfactant/polymer systems. Therefore, surfactants and polymers used to generate graphene/polymer nanocomposites are usually borrowed from the field of CNT/polymer nanocomposites. A prior study in CNTs/polymer nanocomposites has introduced the concept of CNT-philic groups for surfactants that are active at CNT surfaces [83, 84]. Similarly, applying this concept to graphene-compatible surfactants results in “graphene-philic” groups. This article is not an attempt to review the immense literature that exists on graphene/polymer nanocomposites [34, 85, 86]. Rather, there is focus on those nanocomposites prepared using latex technology, with particular regard on the current graphene-philic surfactants and stabilization of graphene/polymer matrix systems. Emphasis

is placed on surfactant and polymer architecture and type to provide a framework for future surfactant selection and design.

2. Graphene-compatible surfactants

A major drive towards the water-borne dispersion of graphene into polymer matrices is to eliminate the use of VOCs. In water, however, the hydrophobic nature of graphene leads to the agglomeration of graphene sheets into graphitic layered structures or agglomerates, thus spontaneous wetting by water is theoretically impossible. It has long been established in colloid science that to achieve a thermodynamically stable dispersion of one phase in another requires the lowering the interfacial energy between two immiscible phases, using surfactants that either strongly bind to the target compound or are solvated by the continuous phase [87-89]. However, very little is known as to whether graphene dispersions can be thermodynamically stable [90]. An analysis of thermodynamic factors important for graphene dispersion can also be found in the review by Texter [91]. Note the similar hydrophobicity between graphene and CNTs; it can be estimated that the increase in entropy on mixing graphene in any solvent would be small or even negative, as it is for CNTs. To achieve a negative free energy of mixing, a suitable solvent that leads to a very small enthalpy of mixing and fully exfoliated graphene sheets should be found. However, graphene dispersed in surfactant solutions can often remain stable over long periods of time. As with many colloidal systems (e.g. emulsions), although the dispersions may be thermodynamically unstable, one can rely on the kinetic stabilization resulting from the electrostatic and steric barriers provided by the adsorbed surfactants on the graphene sheets to prevent destabilization of dispersed graphene.

Compared to surfactant stabilized CNT/polymer systems, surfactant assisted graphene/polymer nanocomposites have not yet been fully explored. This is partially due to

the lack of fundamental information about the properties and intermolecular interactions of this new material. Currently, a variety of surfactants including ionic, nonionic and polymeric surfactants have been used to stabilize graphene/polymer systems via latex technology. It is conceivable that different surfactant types would likely operate with different stability mechanisms in graphene + polymer matrix systems. Each type of surfactant will be reviewed in the following sections, and the chemical structures for the studied surfactants are given in Table 1.

2.1 Ionic surfactants

Ionic surfactants have traditionally been the preferred choice for carbon family/water dispersions [92-95]. Owing to the good compatibility between ionic surfactants and carbon materials, this type of surfactant has been the main focus of investigations into graphene dispersions. Sodium dodecylsulfate (SDS), sodium dodecylbenzenesulfonate (SDBS), and cetyltrimethylammonium bromide (CTAB) are surfactants most frequently used to improve the dispersion of CNTs [96, 97], and, more recently, graphene [60]. Also investigated was the use of bile salt biosurfactants (sodium cholate (SC) surfactants) [57]. All the selected surfactants exhibited graphene-compatibility and have been widely employed in studying graphene dispersion in water, as well as to stabilize colloidal systems consisting of graphene and polymer matrices.

The use of the anionic surfactant SDS (compound 1, Table 1) in the preparation of PMMA (compound 1 Table 2) reinforced functionalized graphene (FGN) nanocomposites was reported by Jiang and co-workers [98]. One preparation method, that includes the role of surfactant is called latex technology plus melt blending (composite 1), and another which does not is called direct melt blending (composite 2). Unlike composite 1, composite 2 suffers significant agglomeration and cannot attain the same dispersion level or reinforcing

effectiveness as SDS stabilized FGN/PMMA nanocomposites. Aguilar-Bolados et al. [61] also showed that graphene with surfactant coatings are distributed uniformly and arranged interstitial latex particles, as observed using transmission electron microscopy (TEM). The results suggested that the presence of SDS on the graphene surfaces enables favorable interfacial interactions between SDS coated graphene and the host polymer matrix, enabling high particle-to-matrix-to-particle loading. It is the hydrophobic interactions which cause significant adhesion between alkyl tails and graphene surfaces in water [99]. The low solubility of alkanes in water would suggest the dodecyl tails of SDS interact and wrap onto the graphene surfaces, preventing water to reach the sheet surface and hence impeding aggregation. Jiang et al. [97] used Fourier transform infrared (FTIR) and Auger electron microscopy (AES) to prove the presence of surfactant tails adhered to the nanotube surfaces. It is worth mentioning the ideal scenario, where alkyl tails would cover the graphene surfaces such that all the graphene sheets were fully separated into monolayer sheets: practically however this is unattainable. Recent studies by Hsieh et al. [100] and Glover et al. [101] pointed out regions where adsorption does not occur – SDS does not adsorb onto regions containing other functionalities e.g. oxygen as in graphene oxide (GO) and the reduced form, reduced graphene oxide (rGO). In this case, the exfoliated state may not produce exclusively monolayer sheets, but instead few layer graphene (FLG) or even stacked graphene may exist.

Practical results have also been achieved using SDBS to produce polymer reinforced graphene nanocomposites. SDBS (compound 2 Table 1) has proven to be efficient at separating CNTs and dispersing them for composite processing [58, 60]. Stable dispersions of graphene in water were achieved using this surfactant as reported by the Coleman group [60]. Centrifugation of 0.1 – 10 mg/mL “crude” graphene dispersion using 0.5 to 10 mg/mL SDBS resulted in actual graphene dispersions in the range of 0.002 – 0.050 mg/mL (see Table 3). Despite the very low dispersion levels, they provided a framework in the surfactant-stabilized

graphene dispersion. One unique property that distinguished SDBS from SDS is the presence of a phenyl ring near the hydrophilic group. An interesting simulation study, carried out by Suttipong et al. [102] noted that the phenyl rings positioned in a close proximity with the nanotube sidewalls along with the surfactant tails, while the hydrophilic moieties oriented toward water for dissolution. This may explain why SDBS often outperformed the dispersing power of SDS. It is pertinent to note that this proposed arrangement occurred at low concentrations where the surfactant molecules can adsorb randomly onto the graphene sheet. The synergistic effect of aromatic ring through the π - π interactions with the electron-rich of π -conjugated systems may offer more favorable interactions between surfactants and graphene sheets, hence improving the dispersion of graphene in water and subsequently in the polymer host [58, 60, 103]. Work by Ghislandi et al. [38] reported the use of SDBS at concentrations above its cmc to counterbalance the van der Waals interactions between graphene sheets to make nanocomposites with polypropylene. Scanning electron microscopy (SEM) images give evidence that, without surfactant, graphene sheets were highly wrinkled or folded into fluffy structures (see Fig.2d.) due to strong inter-sheet interactions. Addition of SDBS to the system promotes individualization of the graphene sheets. However, the extent of exfoliation is limited; there are still some signs of re-stacking or folding of the sheets inside the polymer matrix (Fig.2f.).

In a subsequent study, nanocomposites were obtained using a different anionic surfactant, sodium cholate (SC, compound 3 Table 1). This surfactant may prefer to lie flat on a graphene surface with more hydrophilic hydroxyl and carboxyl groups oriented toward the aqueous phase. Simulation studies confirmed that planar SC molecules partially cover 60% of the graphene surface and are adsorbed parallel to the graphene surface to maximize the hydrophobic interactions [104, 105]. However, the computed adsorption still falls short of the value reported by Green et al. [106] estimating that 94% of the graphene surface is occupied

by SC molecules. Shahil and Balandin [78] used ~46.45mM of sodium cholate solution to exfoliate natural graphite using high power ultrasonication. Although stereochemically the surfactant may favor stronger interactions with the graphene surface (as compared to SDS and SDBS), the resulting dispersion did not consist entirely of single layer graphene, but a co-existing distribution with multilayer graphene (MLG). A study on graphene dispersion using SC was also reported by Tkalya et al. [28]. They presumed that the graphene dispersions do not fully consist of single layer graphene, noting the presence of clusters in the final composites. Interestingly, the chosen surfactant concentrations for producing graphene via liquid-phase exfoliation were 0.1 and 1 mg/ml which is far below the cmc of SC itself (~5 mg/ml).

An initial dispersion study using this surfactant reported that in the applied concentration range, lower surfactant concentrations provided higher dispersion ability and stability than concentrations close to the cmc [57]. The discrepancy remains unresolved. A similar increase in dispersed nanomaterial with lower surfactant concentration was observed by Jiang et al. [97] and Bystrzejewski et al. [107] for the case of CNT dispersions using SDS and SDBS. They noted that it was possible to obtain stable and highly concentrated nanotube dispersions at surfactant concentrations below cmc, although the authors did not conclude on the mechanism.

Despite a plethora of work on ionic surfactants, there is still a dearth of literature on the exfoliation and dispersion of graphene using cationic surfactants. Cationic surfactants, specifically cetyltrimethylammonium bromide (CTAB, compound 4 Table 1), were utilized in the earliest model for studying surfactant aggregation on highly ordered pyrolytic graphite [108]. The mechanism of how this surfactant adsorbs on the graphite surface can be found elsewhere [108, 109]. Following the exfoliation technique introduced by Lotya et al. [60], Notley and Griffith [110] have studied the effect of CTAB concentration (0.1 – 0.9 mM) on

the yield of graphene exfoliated from graphite (see Table 3), with the highest graphene dispersion achieved at a surfactant concentration of 0.7 mM; slightly below its cmc (around 0.9 – 1.0 mM) with the surface tension of CTAB solution approximately 40 mN m^{-1} . Wang et al. [111] also suggested that CTAB helps to match the surface energy between graphene and water for a dispersion, which they claimed was stable for 15 days. However, the studies were limited to the measurement of CTAB surface tension, rather than surfactant-stabilized dispersions of graphene. When applied to a mixture of graphene and a polymer matrix, Kim et al. [112, 113] demonstrated that quaternary ammonium salt CTAB (at its cmc) was able to modify the dispersibility of MLG in water to prepare nanocomposites of styrene butadiene rubber (SBR, compound 3 Table 2). The results revealed that CTAB-stabilized MLG is far more effectively dispersed in the SBR matrix than the raw MLG. The zeta (ζ)-potential was used to characterize the dispersion state of the system. The positively-charged CTAB solution imparts an effective charge on MLG sheets enabling them to interact electrostatically with the negatively-charged SBR particles (see Fig.3.) to give a uniform filler dispersion. A parallel approach, but with a different polymer, was undertaken by Matos et al. [44], here TEM elemental mapping of nitrogen was used to show that CTAB adhered preferentially at the edges of the rGO sheets and coalesced rubber. The ability of surfactants to alter interfacial energy is one of the driving forces for the migration towards the interface during film formation [114]. This characteristic was proposed to be an important factor for the interaction between filler and polymer matrix.

2.2 Nonionic surfactants

Nonionic surfactants contain non-charged highly polar moieties which are usually dominated by polyoxyethylene (poly(ethyleneoxide)) hydrophilic groups. Technical grade nonionic surfactants such as Triton X-100 (compound 5, Table 1) and Pluronics (also

containing hydrophobic poly(propyleneoxide) blocks) are polydisperse in the number of oxyethylene groups and contain trace impurities. Stabilization resulting from these surfactants invoke repulsions which occur between nonionic macromolecules dissolved in the aqueous phase and is generally termed steric stabilization (see Section 4.1). Yoonessi and Gaier [42] have utilized Triton X-100 to produce graphene nanosheet/polycarbonates (PC, compound 4 Table 2) nanocomposites. The results showed that the surfactant helped graphene particles to assemble and position throughout the matrix which therefore provided a conductive path for electron transport to generate a conductive polymer. Comparisons between the same materials but with different techniques *i.e.* solution mixing showed that the latex technique gives a more substantial improvement in electrical properties, resulting from the uniform dispersion of filler. Later, Wan et al. [115] examined the ability of this surfactant in a system containing thermally reduced graphene oxide (TRGO) and epoxy resin (compound 5 Table 2). It was claimed that non-covalent functionalization with Triton X-100 above its cmc (see Table 4, cmc Triton X-100 = 0.02 mM at 25°C) helped to maintain the dispersion stability for over a month, whereas the pristine graphene suffers from rapid sedimentation. Control of dispersion quality, via hydrophilic-hydrophobic bridging of the adsorbed surfactant, is believed to be a substantial factor. The presence of a phenyl ring, which in many disciplines is considered to be favourably “face-to-face” stacked with the aromatic system of graphene, also takes part in providing the enhanced graphene-philicity. Interestingly, phenyl rings combined with branched alkyl tails were also assumed to affect the aggregation pattern of the surfactant on the hydrophobic surface [116, 117].

Pluronics are another group of polyoxyethylene surfactants/block co-polymers used for graphene dispersal in NR-latex. Aguilar-Bolados et al. [61] provided comparison of dispersing ability between SDS and Pluronic F 127 (compound 6, Table 1). They found the resultant composites had a different dispersion quality, with SDS allowing for more

efficiently distributed nanofillers than Pluronic F 127. Nevertheless, comparison between surfactant performance should be made carefully as each surfactant type would give a distinctly different kind of stabilization. The authors posit that the bulky poly(propyleneoxide) chains of Pluronic may impede the surfactant tails from diffusing between graphene sheets for intersheet isolation. Sometimes the hydrophobic size only exerts partial control over the exfoliation [118]. This can be related to the Israelachvili packing parameter, $v_o/a_o l_o$ where v_o is the hydrophobic tail volume, l_o is the maximum extended length of surfactant tail length and a_o is the headgroup area per molecule [119]. The area occupied by a headgroup is determined by the steric interactions between neighboring ethylene oxides that is crucial to the height of steric barrier [116, 117]. Meanwhile, the alkyl tails are decisive to the interaction, geometry and coverage of surfactant monolayer on the surface. However, the importance of the hydrophilic-lipophilic balance (HLB) should be recognized, just as in other colloidal systems [120].

2.3 Polymeric surfactants

With the realization that some amphiphilic polymers are capable of providing a stable dispersion of graphene in aqueous medium [58, 121-123], efforts towards generating graphene/polymer nanocomposites stabilized by amphiphilic polymers have been made. Previously, it has been shown that physically adsorbed block copolymers on CNT sidewalls can enhance the dispersion of CNTs in water and organic solvent [124-126]. The first report of a graphene/polymer nanocomposite prepared using latex technology was achieved using anionic polymer, poly(sodium-4-styrenesulfonate), denoted as PSS (see Table 1 compound 7) [27]. In this study, graphene-coated PSS was synthesized by reducing graphite oxide with hydrazine in the presence of a ten-fold excess of PSS ($M_w = 70\ 000\ \text{g/mol}$). This approach followed on from the success of graphene dispersions reported by Stankovich, who claimed

to prevent the graphene sheets from agglomerating for a year [123]. UV-Visible spectroscopy was used to quantify the dispersion state of graphene, but without supporting data [27]. It is surprising though, that such high molecular weight material should be added in excess to provide a sufficient barrier against agglomeration. For a class of polymeric surfactants, higher molecular weight material might be expected to provide a thicker shell around particles. O'Connell et al. [126] reported that charged polymers such as poly(styrenesulfonate), although capable of dispersing SWNT up to 4g/L, exhibit low binding affinity with the CNT walls and are sensitive to the solution environment. Later Stankovich et al. [123] reiterated this hypothesis. The authors mentioned that the large amount of PSS was needed to compete against agglomeration during deoxygenation of graphite oxide. The uniform dispersion however does not constitute a great enhancement in the composite electrical properties. The excess PSS in the final composite was assumed to overshadow the inherent electron transport of the graphene network. Tantis et al. [62] used amphiphilic block copolymers (compound 8 Table 1) to generate graphene/PVA nanocomposites. The copolymer-wrapped graphene is more homogeneously integrated within the PVA (compound 6 Table 2) matrix than those solely graphene. The stabilization scenario relies on the ability of one hydrophilic block containing alkylamino and carboxylate to interact with the PVA matrices, whereas the other block remains adhered to the graphene surface [127].

3. Specific applications of surfactant

3.1 Surfactant stabilization: The DLVO theory and steric forces

The stability of colloids is an important subject from both an academic and industrial point of view. Colloidal stability is governed by the balance of repulsive interactions and the relentless van der Waals interactions between particles [128]. In general, a stable dispersion means that individualized graphene sheets can exist in close proximity to each other without

the possibility of aggregation. There are two approaches for preventing colloidal particles from coagulation. One is based on electrostatic repulsion between two charged particles as in the well-known theory due to Derjaguin, Landau, Verwey and Overbeek (DLVO). The other is a non-electrostatic repulsion that occurs in a dilute solution between nonionic molecules to provide steric stabilization [129].

The basis of DLVO theory is the linear summation of the electrical double layer repulsion (V_R) and van der Waals attraction (V_A) at a certain distance (h), where a typical energy–distance curve can be established to describe the kinetic stability of colloidal dispersion [120, 129-131].

$$V(h) = V_A(h) + V_R(h) \quad (1)$$

It is the potential energy barrier $V(h)$ which can provide the mechanism for stability of charged colloidal particles. The higher $V(h)$ value will pose a suitable barrier to aggregation and thus the longer system will remain stable, but when the barrier is low, the colloidal systems lose stability. The height of the electrical double layer barrier is determined by the surface potential of Stern layer – zeta (ζ)-potential and the thickness of double layer [60, 128, 132]. The universally accepted condition at which colloidal system classified as “stable” is when (ζ)- potential larger than +40 mV or less than -40 mV [133].

A study by Lotya et al. [60] using anionic SDBS (compound 2 Table 1) showed that ζ -potential of the fresh graphene dispersion stabilized by SDBS was measured to be -44 mV (see Fig.4A.), which indicates good dispersion stability. As shown in Fig.4C., the nearby graphene sheets experience a larger potential barrier (V_T), and stems from the electrostatic potential $2V_{DLVO}$ of two charged graphene sheets which suitably outweigh the van der Waals interactions, V_{vdw} . The calculated van der Waals interaction potentials, expressed in terms of the Hamaker constant, for graphene in vacuum and water [134] are 9×10^{-21} J and 13×10^{-21} J

respectively, whereas for graphene oxide [135] it is 2.37×10^{-21} J. The height of the V_T therefore controls the stability surfactant-coated graphene sheets dispersion. Recently, Smith et al. [77] also investigated the stability of an extremely dilute graphene dispersion using a large variety of ionic surfactants (see Table 3). They suggested that to obtain a higher fraction of dispersed graphene, it is necessary to increase the ζ -potential or the EDL thickness, in other words increasing the surface charge density of graphene surfaces. At this point, surfactants that pack tightly onto the graphene sheets are needed. This is because tuning the charge density of a surface normally leads to an increase in adsorption of charged compounds.

The steric stabilization involves covering the colloidal particles with a dense polymer layer. The mechanism arises from the “brush-to-brush” contact of the polymer chain layers when these are in a suitable solvent and the loss of entropy of the chains on significant overlap. If the interaction between the chains is greater than the solvent-chain interaction, then rather than repulsion, attraction between adjacent particles may occur, leading to coagulation. To ensure an effective steric stabilization, it is best if the stabilizing chains are highly soluble in the medium, while the insoluble chains are strongly adsorbed to the particle surfaces for complete coverage. As in the DLVO theory, the total energy of interaction will be the sum of attractive and repulsive steric interactions [128, 129, 133]. This steric stabilization is usually provided by nonionic surfactants or polymer (ionic or nonionic).

Using four nonionic surfactants; Tween 20, Tween 80, IGEPAL CO-890 (compounds 9-11 Table 2, respectively) and Triton X-100, Smith et al. [77] studied the relationship of steric barrier energy and the stabilization of aqueous graphene dispersions (details on the graphene dispersions can be seen in Table 3). The results highlight that the steric energy barrier is closely related to surfactant molecular weight, and thus surfactants with higher molecular weights are expected to result in more colloiddally stable graphene. The reason is

that the surfactants are likely to have longer hydrophobic chains and provide thicker layers between adjacent dispersed particles [120]. They also concluded that longer and more polar headgroups would render the surfactant graphene-philic due to the stronger interaction with water. Recently, Seo et al. [118] reported that increasing the hydrophilic group polarity, by increasing the oxyethylene number for Pluronic surfactants (general structure of Pluronic can be seen in compound 6 Table 1) resulted in higher potential barriers. Thus, Pluronics with longer polypropylene oxide (PEO) segments are more effective at providing stable graphene dispersions. Unlike the PEO segments, the trend of increasing graphene affinity for the hydrophobic polypropylene oxide (PPO) portions do not always follow a simple pattern. There are certain limits that should be taken into account, because a very long PPO may ‘overkill’ the ability of the surfactant chain to diffuse between graphene sheets during intersheet separation. For the family of Tetronics (structure 12 Table 1), the trends are more subtle, though they provided higher dispersion efficiency than all Pluronic surfactants considered. Interestingly, a recent simulation study utilising the anionic surfactant sodium cholate as a model surfactant suggested that steric repulsion exists between the sodium counterion wall and the single layer of adsorbed cholate ions two confined graphene sheets, thus preventing aggregation [105]. Note that for charged colloids, typically electrostatic repulsions contribute to the stable dispersion of the colloidal system.

3.2 Dispersion mechanism: surfactant-graphene interaction

Little is known about the molecular details of the interactions between surfactant molecules and carbon nanomaterials (especially graphene) including the correlation of these interactions with the surfactant assisted colloidal stability. A major hindrance in processing graphene is the mutual attraction between adjacent graphene sheets due to van der Waals interactions. These types of attractive interactions are always present, but their intensity can

be modified by dispersion in surfactant solution [77, 93, 105, 136]. The presence of surfactant hydrophilic groups renders them soluble in water in a similar manner with graphene oxide but without unduly perturbing the unique properties of graphene [137].

It is well established that dispersions of graphene in aqueous surfactant solution largely rely on the use of external energy i.e. ultrasonication [93]. Dispersions coupled with sonication promote exfoliation to generate individual carbon nanomaterials. It is pertinent to note that long exposure of high power ultrasonication can induce defects on graphene sheets which are detrimental to the final composite properties [57, 60]. The high shear caused by ultrasonication induces the peeling of the outer parts of aggregates, thus providing new adsorption sites for the surfactant tail onto the nanomaterial sheets.

Extensive studies on surfactant self-assembly at hydrophobic materials led to conclusions that there are two major factors exerted by the surface to the self-assembly structures of the adsorbed amphiphilic compounds [108, 117, 138]. First, is the affinity of the alkyl tails to the surface which is driven by the minimisation of graphene/graphite-water interfacial energy as a result of hydrophobic interactions. The second is a preferred orientation of the alkyl chains with the surface lattice because the carbon position in the alkyl chains is closely matched with the graphene surfaces [105, 108, 116, 117, 138, 139].

Studies revealed that there are two models considered for the alkyl tail orientation on the graphite surface; the chains may lie flat or stand perpendicularly to the basal plane of graphite [117, 140-142]. The earliest study of surfactant aggregation on graphite proposed that surfactant molecules initially adsorb with their alkyl chains extended on the graphite surface [108]. On increasing the surfactant concentration, the alkyl chains gradually stand perpendicularly with the hydrophilic group facing toward the aqueous medium. Using nonionic disaccharide surfactants, Holland et al. [140] demonstrated that the adsorbed surfactant tails lie along the graphene sheets. Later, Yin et al. revealed that the distances

between surfactant chains and the basal plane of graphite are 3.8 Å and 3.7 Å, and 4.5 Å for the flat and perpendicular orientation, respectively [141]. It was postulated that the flat orientation is more favorable because there are more carbon atoms in close proximity maximizing interaction with the graphite surfaces. Meanwhile, the perpendicular orientations have higher chain-chain interactions, and thus lead to fewer graphite-alkane chain interactions. They also noted that the interactions between methylene groups and graphene sheets are dominated by van der Waals interactions, and that the electrostatic interactions are negligible.

For non-aromatic surfactants, Grant et al. [139] and Patrick et al. [116, 117] suggested that there is a correlation between the number of methylene units in the alkyl tails and the ability of the compound to self-assemble onto the graphite surface. Holland et al. [140] also noted that the surfactant self-assembly structure is determined by the alkyl chain length. The proposed hemicylindrical micelle radius and the area occupied by one surfactant molecule were found to decrease with shorter alkyl chain lengths. This is because surfactant hydrophobicity is known to increase logarithmically with the number of carbon atoms in the hydrophobic chain and usually fits the Klevens equation (eq 2) for linear single-chain surfactants [143], where A and B are constants for a homologous series and n_c is the number of carbon atoms in the surfactant chain. The values of A and B vary with the charge and type of headgroup and additional one carbon atom of $-\text{CH}_2$ group.

$$\log(\text{cmc}) = A - Bn_c \quad (2)$$

This is also true considering arguments based on the packing density of the adsorbed surfactants [85, 115, 116, 125].

If graphene is considered as a large polyaromatic carbon molecule with an electron rich aromatic ring, the surface affinity can also be enhanced via π - π interactions between the

aromatic rings of the surfactants and the graphene. Molecules containing aromatic rings are proven to have a relatively high affinity for carbon nanomaterials e.g. CNT adsorbed more phenol than cyclohexanol from water, where the magnitude π - π interactions was suggested to depend on the size, shape and number of the aromatic units [144-149]. An increasing number of studies also note that the size of the aromatic system plays an essential role in increasing the affinity of molecules to graphene surfaces [145-147, 149, 150], but unfortunately most reported surfactants have relatively few aromatic moieties.

The π - π interactions infer face-to-face stacking (see Fig.5A) of the surfactant containing aromatic ring(s) and the graphene basal planes involved in the non-covalent interactions [151], although the nature of this remains controversial [152, 153]. It is not really well understood why the basal plane of graphene is more interacting than the graphene edges, and evidence is limited on modelling and scanning tunneling microscopy (STM) studies [146, 148, 154-156]. One plausible reason is that the number of defects in graphene edges may be quite high in comparison to the basal plane sites [157]. In addition, non-covalent functionalization is acknowledged to be effective on the specific plane of graphene, but is unsuitable for graphene edges which are commonly used for direct functionalization [158]. These π - π interactions are often referred to as an “aromatic donor-acceptor interactions” [159-161], but others reached different conclusions. Hunter et al. [162] and Waters [163] suggested that it is not the sheer presence of donor-acceptor interactions alone that is decisive, instead they are more complex and consist of electrostatic, hydrophobic and van der Waals interactions. A recent theoretical study by Björk et al. [151] concluded that the assumed π - π interactions may be a combination of dispersive and electrostatic forces, in which the dispersive forces responsible for the affinity of the adsorbed molecules toward graphene surface, whereas the electrostatic interactions provided stability for the complex unit.

The addition of phenyl groups on the surfactant chains is also known to increase the overall hydrophobicity of the AOT-analogue surfactant [164]. Thereby, increasing hydrophobicity of the molecules may also lead to enhanced interactions between molecules and graphene surfaces. This is corroborated by Wang et al. [150] as their study involving pyrene, naphthalene and phenanthrene adsorption on graphene nanosheets shows. Here, they show that hydrophobicity does play a role in the affinity of the aromatic series towards graphene. The adsorption of these molecules onto graphene sheets increased linearly with increasing hydrophobicity, following the order of pyrene > phenanthrene > naphthalene. With the assumption that the aromatic molecules are in a face-to-face arrangement with the graphene surfaces, then the total adsorbed amount of each molecule for naphthalene, phenanthrene and pyrene are 114.0; 116.0; 123.1 mg/g respectively. The existence of π - π interactions between aromatic molecules and graphene was evident using FTIR spectroscopy. The corresponding peak for C=C bonds of the aromatic rings on graphene nanosheets shifted from 1627 to 1633, 1639, and 1637 cm^{-1} after adsorption of naphthalene, phenanthrene and pyrene, respectively. Much earlier, Galbraith et al. [154] studied the adsorption of a series sulfonated dyes onto graphite. They concluded that the affinity of sulfonated dyes toward graphite decrease with increasing number of sulfonate groups on the compounds – increasing hydrophilicity.

An and co-workers [137] recently demonstrated the successful dispersion of graphene assisted by polyaromatic pyrene derivatives namely 1-pyrenecarboxylic acid. They found that water is a prerequisite as an intervening medium to lower the potential interactions between graphene sheets during exfoliation. The effect of different stabilizers containing aromatic groups has also been investigated by Parviz et al. [58], in which graphite exfoliation was assisted by surfactant (SDBS), polymer (PVP, compound 7 Table 2) and pyrene derivatives. They found that commercially available pyrene derivatives were much more efficient for

obtaining higher graphene dispersions (1 mg/mL) at just half the concentration required for SDBS. Pyrene derivatives offer a richer electron environment than the lesser π -conjugated systems on surfactants and polymers, thus enabling them to strongly interact with graphene surfaces. For development applications, raw material costs need to be considered, which, unfortunately, represents a drawback of these pyrene derivatives. At current market prices, their cost is estimated at around 100 – 200 USD per gram using a scientific supplier.

The π - π stacking between graphene and pyrene derivatives can also be altered by attaching polar functional groups to induce temporary polarization in the corresponding molecules. Zhang et al. [103] synthesized and evaluated the performance of two kinds of naphthalene derivatives (see compound 15 Table 1), namely, *N,N'*-bis-[2-(ethanoic acid sodium)]-1,4,5,8-naphthalene diimide (NDI-1) and *N,N'*-bis-[2-(ethanesulfonic acid sodium)]-1,4,5,8-naphthalene diimide (NDI-2) to separate and keep it as individualized sheets in dispersion. Adsorption free energies calculated from periodic density functional theory indicated that larger aromatic molecules (a naphthalene derived surfactant) possessed a stronger affinity towards graphene as reflected by the larger negative free energy of adsorption than those on SDBS or 1-pyrenesulfonic acid sodium salt. Studies by the Sax group [12, 165] provided insights into this aromatic size effect. They suggested that the maximum adhesive interactions between solubilizer and graphene need to be considered in order to peel the material from the agglomerated structure. Adhesion was favored by increasing the molecular size of aromatic groups, meaning that the larger aromatic groups attach more strongly to the graphene surface than the smaller ones, thus efficiently separating them from the stacked form.

3.3 Simulation of surfactant self-assembly on graphene

Adsorption and the resulting self-assembly structure of surfactant on graphene or carbon nanomaterial surfaces has been proposed to give a variety of different morphologies. The most probable structures have been postulated: cylindrical, random monolayer, hemicylindrical and hemimicelle. However, yet again, it has not been fully explored. Thus far, direct evidence supporting self-assembled structures is limited and still remains an open question.

Simulations on SDS carried out by Domínguez et al. [166] proposed that initially surfactant molecules adsorb on graphene randomly to form rough monolayers. At concentrations about one quarter of the cmc, the surfactant aggregates into hemicylindrical structures. On increasing the surfactant concentrations further, graphene monolayers are already completely covered with SDS micelles and rearrange themselves until they have a stable structure *i.e.* cylindrical. Later, Tummala et al. [167] revealed that the self-assembly structure also varied depending on the graphene size and shape. On expanding the literature of anionic surfactant aggregation, simulation on SDBS (a structural relative of SDS) was done by Sun et al. [168]. Initially, SDBS adsorbed in a parallel arrangement with a self-assembled monolayer structure, whereas at high concentrations hemimicelle aggregates formed (see Fig.6.). The surfactant headgroups organized next to the edge sections of graphene sheets in order to maximize contact with water.

Srinivas et al. [138] have carried out molecular dynamics simulations of two nonionic surfactants n-alkyl poly(ethylene oxide), C12E5 (compound 13 Table 1) and C10E3 (compound 14 Table 1) on graphite-like surfaces. They showed that initially surfactants adsorbed with the tails approaching the graphite surfaces, and form a random configuration to begin wrapping the graphite. Once the surface is saturated by surfactant molecules, surfactant monomers in bulk solution start to self-assemble to form micelles. They proposed a “feeding

mechanism” by which the micelles in bulk solution adsorb onto the graphite surfaces and reorganize to provide a more stable conformation. The results indicated that surfactants favor certain arrangements which depend on the alkyl chain length. Surfactants with shorter ethylene oxide units and alkyl tail (C10E3) formed a monolayer, whereas a hemicylinder structure was found for the longer C12E5.

Other simulations using n-alkyl poly(ethylene oxide) have recently been published by Wu and Yang [169]. Here, they provided a larger view of the effect of alkyl chain length and ethylene oxide units to the aggregated structure. The results revealed that as the hydrophobic chain length increases, a hemicylindrical shape starts to emerge and the volume of hemicylinder increases, indicating that a longer tail produces a larger spatial volume of the self-assembly. The radius of the hemicylinders was also found to increase as the headgroup elongated, and thus provides more stable dispersions.

4. Polymers

4.1 Hydrocarbon polymers

Composites based on polymer matrices filled with reinforced nanofillers are very promising candidates for the production of materials with tuneable properties. Latex technology offers a wide range of choice with respect to the polymer matrices. Polymers may be produced from conventional emulsion polymerization or used directly in an emulsion form. The simplest and most ubiquitous polymers used are hydrocarbon polymers which consist entirely of carbon and hydrogen atoms in the polymer backbone. Two kinds of hydrocarbon polymers are currently used for producing graphene/polymer nanocomposites via latex technology, namely saturated and unsaturated hydrocarbon polymers. Saturated hydrocarbon polymers have no double bonds, and thus make it very stable and difficult to deform. Meanwhile, unsaturated hydrocarbons contain double bonds between some carbon

atoms and their neighbors, which are expected to favor direct interaction with graphene surfaces via π - π interactions.

A number of studies have reported the use of the saturated hydrocarbon polymer polypropylene (PP, compound 8 Table 2) to make electrically conductive nanocomposites. Syurik et al. [170] reported that when incorporated into PP matrices, graphene substantially improved the electrical conductivity from 10^{-9} S cm⁻¹ to 4×10^{-3} S cm⁻¹ with 2.0 wt % graphene loading and a percolation threshold at around 0.4 wt% (see Table 4). Observations using scanning electron microscopy (SEM) revealed graphene sheets oriented preferentially in the direction parallel to the PP surfaces to form conductive networks. Ghislandi et al. [38] demonstrated that the large surface area of graphene is beneficial to properly organize inside the polymer matrix helping to increase the conductivity of the final composites. Although encouraging, no plausible interactions between polymer and graphene were suggested to support the reasoning behind the choice of polymer used in this study.

The hydrocarbon polymer polystyrene (PS, compound 9 Table 2) was amongst the first materials to be investigated for graphene/polymer nanocomposites based on latex technology [27]. Studies on CNT/polymer nanocomposites have provided important pointers to make conductive nanocomposite systems using this type of polymer [69, 70, 171-173]. Building on those extensive findings, similar results are expected for polymer reinforced graphene and thus research on graphene/PS nanocomposites is mostly centered on the production of conductive nanocomposites [27, 28, 170, 174, 175]. The presence of π -conjugated systems in the polymer chains would likely favor the filler-to-matrix-to-filler electron transfer between the electron rich system of graphene and the PS matrix. As reported by Tkalya et al. [27], the presence of graphene in PS materials reinforces them, and improves the electrical conductivity to about 0.15 S cm⁻¹ for 1.6 – 2 wt% graphene compared to the initial intrinsic conductivity of polystyrene 10^{-11} S cm⁻¹ (Table 4). A low percolation

threshold was measured in the range of 0.8 – 0.9 wt%. This study further noted that the electrical enhancement of the final composite can be strongly affected by polymer molecular weight. Work by Grossiord [176] noted that PS with a higher molecular weight would have a higher surface tension than those with low molecular weight, thus low molecular weight PS is expected to favorably adsorb to the CNT surfaces to give improved wetting on the surfactant coated CNTs. Although this work provided important pointers, there was no immediate follow up to the graphene/polystyrene nanocomposite; studies on graphene/polymer nanocomposites used the high molecular weight polystyrene (molecular weight 944 kg mol⁻¹).

Natural rubber (NR) is another example of unsaturated hydrocarbon polymer that has been widely studied for polymer reinforced either CNTs or graphene, recently. This biodegradable material shows an interesting both physical and chemical properties and is pervasively used for manufacturing a wide variety of industrial products especially tires. Freshly tapped NR latex from *Hevea brasiliensis* is obtained as a colloidal system of rubber particles dispersed in an aqueous serum [177]. It is generally agreed that NR is composed primarily of a cis-1,4 polyisoprene surrounded with a biocomplex of protein-phospholipid layer (Fig.7a) [177-179]. Recently, work by Nawamawat et al. [178] revealed that NR particles are present with core-shell like structures, and polyisoprene units present as a hydrophobic core encapsulated by a mixed of 84% protein (positively charged) and 16% phospholipid (negatively charged) domains located on the surface to render them hydrophilic (Fig.7b). Protein resides as a major constituent of the latex particle surfaces and thus is considered to be an important component for the stable colloidal dispersion of NR. A recent study by Mohamed et al. [84] has suggested that in colloidal systems consisting of CNTs, NR latex and surfactant, the hydrophilic part of NR-latex would interact favorably with surfactant headgroups, whereas the surfactant tails adsorb onto the CNT surfaces, resulting in

homogeneous dispersions after ultrasonication. More recently, Matos et al. [44] reported that the strong electrostatic interactions of negatively charged NR particles and positively charged CTAB coated graphene contributed to the significant improvement of the composite final properties. That CTAB is distributed at the edges of graphene sheets is one factor that solves the graphene – NR matrix incompatibility. This allows for the formation of graphene networks inside the NR matrices. Thus, making the resulting nanocomposites conductive. Aguilar-Bolados et al. [61] also reported the significant elastic modulus and mechanical strength improvement (see Table 5), proposed to be caused by the incorporation of graphene within the interstices of NR particles due to the formation of nanofiller networks.

Polymers with two different repeating monomers known as copolymers are also used for latex technology. One promising candidate is Styrene Butadiene Rubber (SBR) which is formed by concomitantly reacting monomers of styrene and butadiene together. Practical applications of SBR in manufacturing are tires, footwear, hoses, and conveyor belts. This material, however, suffers from poor thermal and electrical conductivity thus limiting potential applications. Therefore, addition of graphene is expected to enhance their properties. Kim and co-workers [112, 113] report on the efficient dispersion of CTAB-stabilized MLG into SBR matrices; both of which are having different surface potential charge, to render the composite conductive. The presence of a π -conjugated system contributed by the styrene monomers and butadiene double bonds inside the SBR structure is also of importance for the interaction of polymer and CTAB-stabilized MLG. This gives rise to a six order of magnitude electrical conductivity improvement, even at low nanofiller contents ($\sim 10^{-13}$ to 8.24×10^{-6} S cm⁻¹), a slight improvement in thermal stability was also reported (Table 4 and 5).

4.2 Oxygenated polymers

An important development has been achieved through the inclusion of other atoms i.e. oxygen as hydroxyl pendant groups in PVA, or located along the backbone as a C–O or C=O bonds. Tantis and co-workers [62] investigated the reinforcement effect of graphene on PVA matrices. The interesting aspect of this semicrystalline polymer is that property changes associated with polymer crystallinity are seen with graphene addition, allowing to clearly identify the effect of nanofiller content on the polymer crystalline structure. The polymer, PVA present as beads and thus should be heated at 90°C in distilled water to achieve liquid form. As confirmed by X-ray diffraction (XRD) and differential scanning calorimetry (DSC), addition of graphene was found to increase the crystallinity of the final composite than on pure PVA. The difference arises presumably due to immobilization of polymer chains by hydrogen and/or hydrophobic bonding with intercalated graphene at the interface thus lessening the PVA-like properties. A slight thermal property enhancement credited to the incorporated nanofiller was also reported, although the “magical” switch from insulating to highly conductive was not achieved in this study.

Other work published by Yoonessi and Gaier [42], describes polymers containing carbonyl groups in the polymer backbone, namely polycarbonate (PC). Polycarbonate is one thermoplastic polymer with outstanding thermal and mechanical properties to be applied as air-vehicle components [180]. Those fabricated by latex technology again outperformed the systems generated by solution mixing; with the electrical percolation threshold reported at ~0.14 vol% (see Table 4), notably lower than that of solution mixing (~0.38 vol%). The results are reinforced in electrical and mechanical properties within graphene addition up to 2.2 vol%. Already, with low filler loadings, these composites show conductivity levels which may be suitable for aerospace applications e.g. air vehicle components. SEM images showed

that the graphene sheets are located inside polycarbonate microspheres, with the matrix directly wrapped around the graphene sheets generating a path for electron transport between the two materials. Although the so-called latex technology provided remarkable results, the authors preferred to choose composites prepared with solution mixing to explore in more detail using small-angle neutron scattering (SANS) [42]. Therefore, important information relating to the surfactant-stabilized graphene dispersions such as surfactant self-assembly on graphene surfaces remains unexplored. The SANS data were analyzed with a stacked disk structural model, which showed that graphene domains had an effective radius about 1.7 to 2.7 nm. Because the solution mixing does not involve the use of surfactant, a decrease in spacing between graphene sheets occurs rapidly and leads to aggregated structures.

Another type of polymer used for latex based method is PMMA [98]. PMMA was synthesized via emulsion polymerization of methyl methacrylate monomer (MMA) and is subsequently mixed with SDS coated FGN using a melt blending method. It was suggested that the hydrophilic PMMA linked strongly to the SDS coated FGN sheets to lead thermal stability and tensile strength enhancement within a small addition of FGN (± 1 wt%). The inherited properties of such nanofillers should give a significant impact to enhancement of those properties. They assumed that graphene acts to control the movement of polymer chains at the interface, giving improved interfacial interactions between the two materials.

Epoxide polymers, in particular epoxy resins have also been chosen as polymer hosts for latex technology. These typical thermoset polymers contain aromatic rings and reactive epoxy groups which are expected to provide attractive interfacial interactions with graphene sheets. Shahil and Balandin [78] attempted to improve the thermal conductivity of EPON, epoxy resins based on diglycidyl ethers of bisphenol F by adding surfactant stabilized graphene-multilayer graphene (MLG) into the matrices. This study revealed that addition of graphene-MLG can lead to extremely high thermal conductivity (from $0.201 \text{ W m}^{-1}\text{K}^{-1}$ to 5.1

$\text{W m}^{-1}\text{K}^{-1}$), with enhancement factors around 24 compared to from the neat epoxy resins, but without substantial change in electrical conductivity ($1.4 \times 10^{-9} \text{ S cm}^{-1}$). It was also suggested that those nanocomposites have better prospects to be implemented as thermal interface materials due to significant enhancements, having only low nanofiller loadings, compared to commercially available thermal greases or other filler inclusions. The extraordinary enhancement was attributed to the 2D-geometry of graphene as well as strong energy coupling between graphene and organic molecule electronic structures. Other experimental efforts using epoxy resins were reported by Wan and co-workers [115]. They looked at the effects of addition of surfactant-stabilized graphene to epoxy resins based on diglycidyl ethers of bisphenol A. The differences between the two epoxy resins were based merely the phenols used for the synthesis precursor; bisphenol A and bisphenol F differ by replacing the methyl groups with protons (see Table 2). Graphene reinforced the composite tensile strengths and elastic moduli substantially, whereas the composite thermal stabilities were not notably changed (Table 5).

5. Applications and industrial relevance

With the high industrial demand for composite materials, especially in the fields of transportation and electronic devices, the applications of latex technology as a simple, environmentally friendly and reliable alternative method to produce polymer nanocomposites has already gained significant interest. Clearly, economical aspects are of primary importance for the large production of any materials offered on the commercial market. Today, researchers have been seeking ways to readily synthesize graphene in a large quantities using relatively cheap and abundant bulk graphite [181-183]; at current market prices the raw cost of graphite powder is about 100 USD/kg. There have been some promising results, and thus utilization of graphene for polymeric reinforcement may be a possible way to reduce the

production costs of polymer nanocomposites. The more efficient CNTs are also much more expensive, and the use of graphene potentially allows for comparable enhancement of physical properties at a fraction of the cost [27, 78].

Potential applications of composite-reinforced graphene based on latex technology has recently demonstrated exciting results in improving electrical conductivity at low filler contents, high thermal conductivity, chemical and bacterial resistance (see Table 5). All of these results would surely meet industrial needs for advancing the routes in developing high performance light weight polymer composites (low graphene content) for aircraft components, thermally conductive supports for thermal management in electronic devices and engineering applications such as antistatic and electromagnetic interference [42, 78, 170]. These nanocomposites can also find applications involving solvent, gas and bacterial resistance in biomedical applications, pipelines for petroleum industry and hygiene products [44]. Despite the hype, it should be considered too early to tell if graphene nanocomposites, particularly those with latex technology, will allow the current-lab-scale production to scale up to industrial levels. There are practical barriers to overcome, requiring collaboration between scientists and engineers to optimize the various and exciting commercial uses of these unconventional materials.

6. Conclusions

There has been significant experimental and theoretical effort, aimed to harness the properties of interest in graphene by improving dispersion in polymer matrices using surfactants [27, 28, 42, 115]. It has been recognized that the behavior of surfactants in dispersing graphene is similar to that with carbon nanotubes and other carbon materials [69, 83, 97]. An increase number of graphene/polymer nanocomposites have been synthesized via latex technology. In general, there are two different routes were used to obtain surfactant-

stabilized graphene dispersions, either from graphite as starting material (reduction of graphene oxide in the presence of surfactant and liquid-phase exfoliation) or by simply dispersing the as-synthesized graphene in surfactant solutions using ultrasonication (the duration may vary from minutes to hours). The benefits of employing surfactants in dispersing graphene into polymer matrices are clear. However, the prerequisite amount of surfactant used to stabilize the dispersion has so far been unclear, and needs to be established. Furthermore, advances have been hampered by a lack of reliable predictive models for designing graphene-philic molecules because studies have been restricted to dispersing graphene using commercially available surfactants [104-106, 118]. To overcome this limitation, efforts into design and synthesis should be redoubled to find suitable surfactants that will have potential to transform the latex-based technologies. Four criteria may be identified which effect the efficiency of graphene-philic surfactants:

1. Aromatic rings or double bonds on the surfactant chains are important to enhance favorable tail-graphene interactions via π - π stacking.
2. The tail(s) should be not only “graphene-philic”, but also highly hydrophobic to ensure the formation of thick alkyl layers to prevent aggregation between adjacent graphene sheets.
3. The strength of π - π interactions is dependent on the size, shape, and number of aromatic moieties present on the surfactant backbones.
4. The interactions between surfactant headgroup and polymer matrices must be sufficiently strong to reduce the possible weak interactions with graphene surfaces.

Recent research also points towards the possibility of using ionic liquids as alternatives to produce of stable graphene dispersions. The ionic liquid can be in the form of polymer (polymer ionic liquid) or surfactant [184, 185]. Although limited in number, graphenes made by this approach have been studied as composite nanofillers [186].

With respect to polymer hosts, the presence of such functional groups in the polymer may also improve interactions between the surfactant-coated graphene and the polymer matrix. Concerning “Green Chemistry”, the use of latex technology is particularly interesting, especially if the surfactants are also biodegradable and capable of tailoring the interfacial interactions, but at only low levels. This review has aimed to guide the reader to select appropriate surfactants and polymer matrices, and to compare together recent findings to guide future research directions. This should open the door to optimization of latex technology for industrial chemistry processes, as an economic and environmentally favorable approach.

Acknowledgements

The authors would like to acknowledge National Nanotechnology Directorate Division Research Grant; (NND Grant code: 2014-0015-102-03), Fundamental Research Grant Scheme (FRGS; Grant code: 2015-0155-101-02) and the Universiti Pendidikan Sultan Idris for financial and facilities support. This project was supported by JSPS [KAKENHI, Grant-in-Aid for Young Scientists (A), No. 23685034], and Leading Research Organizations (RCUK [through EPSRC EP/I018301/1], ANR [13-G8ME-0003]) under the G8 Research Councils Initiative for Multilateral Research Funding –G8-2012.

References

1. Geim AK, Novoselov KS, *Nat Mater*, 2007; 6: 183.
2. Novoselov KS, Jiang D, Schedin F, Booth TJ, Khotkevich VV, Morozov, SV, Geim AK, *Proceedings of the National Academy of Sciences of the United States of America*, 2005; 102: 10451.

3. Novoselov KS, Geim AK, Morozov, SV, Jiang D, Zhang, Y, Dubonos, SV, Grigorieva, IV, Firsov AA, Science, 2004; 306: 666.
4. Zhang T, Xue Q, Zhang S, Dong M, Nano Today, 2012; 7: 180.
5. Casiraghi C, Hartschuh A, Qian H, Piscanec S, Georgi C, Fasoli A, Novoselov KS, Basko DM, Ferrari AC, Nano Lett, 2009; 9: 1433.
6. Castro Neto AH, Guinea F, Peres NMR, Novoselov KS, Geim AK, Rev Mod Phys, 2009; 81: 109.
7. Chen Y, Zhang B, Liu G, Zhuang X, Kang E-T, Chem Soc Rev, 2012; 41: 4688.
8. Kane CL, Mele EJ, Phys Rev Lett, 2005; 95: 226801.
9. Haddon RC, Acc Chem Res, 2013; 46; 2191.
10. Loh KP, Bao Q, Ang PK, Yang J, J Mater Chem, 2010; 20: 2277.
11. Sanchez VC, Jachak A, Hurt RH, Kane AB, Chem Res Toxicol, 2012; 25: 15.
12. Lechner C, Sax AF, J Phys Chem C, 2014; 118: 20970.
13. Geim AK, Kim P, Sci Am, 2008; 298: 90.
14. Katsnelson MI, Mater Today, 2007; 10; 20.
15. Lee C, Wei X, Kysar JW, Hone J, Science, 2008; 321: 385.
16. Stoller MD, Park S, Zhu Y, An J, Ruoff RS, Nano Lett, 2008; 8: 3498.
17. Stankovich S, Dikin DA, Dommett GHB, Kohlhaas KM, Zimney EJ, Stach EA, Piner RD, Nguyen ST, Ruoff RS, Nature, 2006; 442: 282.
18. Du X, Skachko I, Barker A, Andrei EY, Nat Nanotechnol, 2008; 3: 491.
19. Nair RR, Blake P, Grigorenko AN, Novoselov KS, Booth TJ, Stauber T, Peres NMR, Geim AK, Science, 2008; 320: 1308.
20. Mao Y, Fan Q, Li J, Yu L, Qu L-b, Sens Actuators, B, 2014; 203: 759.

21. Bae S, Kim H, Lee Y, Xu X, Park J-s, Zheng Y, Balakrishnan J, Lei T, Ri Kim H, Song YI, Kim Y-J, Kim KS, Ozyilmaz B, Ahn J-H, Hong BH, Ijima A, Nat Nanotechnol, 2010; 5: 574.
22. Eda G, Fanchini G, Chhowalla M, Nat Nanotechnol, 2008; 3: 270.
23. Watcharotone S, Dikin DA, Stankovich S, Piner R, Jung I, Dommett GHB, Evmenenko G, Wu S-E, Chen S-F, Liu C-P, Nguyen ST, Ruoff RS, Nano Lett, 2007; 7: 1888.
24. de Heer WA, Berger C, Ruan M, Sprinkle M, Li X, Hu Y, Zhang B, Hankinson J, Conrad E, Proceedings of the National Academy of Sciences of the United States of America, 2011; 108: 16900.
25. Stankovich S, Dikin DA, Piner RD, Kohlhass KA, Kleinhammes A, Jia Y, Wu Y, Nguyen ST, Ruoff RS, Carbon, 2007; 45: 1558.
26. Fernández-Merino MJ, Guardia L, Paredes JI, Villar-Rodil S, Solís-Fernández P, Martínez-Alonso A, Tascón JMD, J Phys Chem C, 2010; 114: 6426.
27. Tkalya E, Ghislandi M, Alekseev A, Koning C, Loos J, J Mater Chem, 2010; 20: 3035.
28. Tkalya E, Ghislandi M, Otten R, Lotya M, Alekseev A, van der Schoot P, Coleman J, de With G, Koning C, ACS Appl Mater Interfaces, 2014; 6: 15113.
29. Pham VH, Dang TT, Hur SH, Kim EJ, Chung JS, ACS Appl Mater Interfaces, 2012; 4: 2630.
30. Potts JR, Shankar O, Du L, Ruoff RS, Macromolecules, 2012; 45: 6045.
31. Moniruzzaman M, Winey KI, Macromolecules, 2006; 39: 5194.
32. Rahmat M, Hubert P, Compos Sci Technol, 2011; 72: 72.
33. Spitalsky Z, Tasis D, Papagelis K, Galiotis C, Prog Polym Sci, 2010; 35: 357.

34. Kuilla T, Bhadra S, Yao D, Kim NH, Bose S, Lee JH, *Prog Polym Sci*, 2010; 35: 1350.
35. Hernández M, Bernal MdM, Verdejo R, Ezquerro TA, López-Manchado MA, *Compos Sci Technol*, 2012; 73: 40.
36. Kim H, Abdala AA, Macosko CW, *Macromolecules*, 2010; 43: 6515.
37. Verdejo R, Bernal MM, Romasanta LJ, Lopez-manchado MA, *J Mater Chem*, 2011; 21: 3301.
38. Ghislandi M, Tkalya E, Marinho B, Koning CE, de With G, *Composites, Part A*, 2013; 53: 145.
39. Huang J-C, *Adv Polym Technol*, 2002; 21: 299.
40. Giannelis EP, Krishnamoorti R, Manias E, In Binder K, de Gennes P-G, Giannelis EP, Grest GS, Hervet H, Krishnamoorti R, Léger L, Manias E, Raphaël E, Wang S-Q, *Polymers in Confined Environment*, Springer Berlin Heidelberg; 1999, pp. 107-147.
41. Alexandre M, Dubois P, *Mater Sci Eng R*, 2000; 28: 1.
42. Yoonessi M, Gaier JR, *ACS Nano*, 2010; 4: 7211.
43. Xing W, Tang M, Wu J, Huang G, Li H, Lei Z, Fu X, Li H, *Compos Sci Technol*, 2014; 99: 67.
44. Matos CF, Galembeck F, Zarbin AJG, *Carbon*, 2014; 78: 469.
45. Rafiee MA, Rafiee J, Wang Z, Song H, Yu Z-Z, Koratkar N, *ACS Nano*, 2009; 3: 3884.
46. Tang H, Ehlert GJ, Lin Y, Sodano HA, *Nano Lett*, 2011. 12(1): p. 84-90.
47. Green AA, Hersam MC, *J Phys Chem Lett*, 2009; 1: 544.
48. Leenaerts O, Partoens B, Peeters FM, *Phy Rev B*, 2009; 79: 235440.
49. Li D, Muller MB, Gilje S, Kaner RB, *Nat Nanotechnol*, 2008; 3: 101.
50. Wang S, Zhang Y, Abidi N, Cabrales L, *Langmuir*, 2009; 25: 11078.

51. Shen J, Hu Y, Li C, Qin C, Shi M, Ye M, Langmuir, 2009; 25: 6122.
52. Kim H, Miura Y, Macosko CW, Chem Mater, 2010; 22: 3441.
53. Zhan Y, Wu J, Xia H, Yan N, Fei G, Yuan G, Macromol Mater Eng, 2011; 296: 590.
54. Cortijo A, Vozmediano MAH, Nucl Phys B, 2007. 763(3): p. 293.
55. Banhart F, Kotakoski J, Krasheninnikov AV, ACS Nano, 2011; 5: 26.
56. Lim H, Lee JS, Shin H-J, Shin HS, Choi HC, Langmuir, 2010; 26: 12278.
57. Lotya M, King PJ, Khan U, De S, Coleman JN, ACS Nano, 2010; 4: 3155.
58. Parviz D, Das S, Ahmed HST, Irin F, Bhattacharia S, Green MJ, ACS Nano, 2012; 6: 8857.
59. Christian Kemp K, Cho Y, Chandra V, Kim KS. In Georgakilas V (editor), Functionalization of Graphene. Wiley-VCH Verlag GmbH & Co KGaA; 2014. Chapter 7, pp. 199-218.
60. Lotya M, Hernandez Y, King PJ, Smoth RJ, Nicolosi V, Karlsson LS, Blighe FM, De S, Wang Z, McGovern IT, Duesberg GS, Coleman JN, J Am Chem Soc, 2009; 131: 3611.
61. Aguilar-Bolados H, Brasero J, Lopez-Manchado MA, Yazdani-Pedram M, Composites, Part B, 2014; 67: 449.
62. Tantis I, Psarras GC, Tasis DL, eXPRESS Polym Lett, 2012; 6: 283.
63. Bryning MB, Milkie DE, Islam MF, Kikkawa JM, Yodh AG, Appl Phys Lett, 2005; 87: 161909.
64. Lagaly G, Appl Clay Sci, 1999; 15: 1
65. LeBaron PC, Wang Z, Pinnavaia TJ, Appl Clay Sci, 1999; 15: 11.
66. Shah RK, Hunter DL, Paul DR, Polymer, 2005; 46: 2646.
67. Fornes TD, Yoon PJ, Hunter DL, Keskkula H, Paul DR, Polymer, 2002; 43: 5915.

68. Grossiord N, Kivit PJJ, Loos J, Meuldijk J, Kyrlyuk AV, van der Schoot P, Koning CE, *Polymer*, 2008; 49: 2866.
69. Yu J, Lu K, Sourty E, Grossiord N, Koning CE, Loos JE, *Carbon*, 2007; 45: 2897.
70. Regev O, Elkati PNB, Loos J, Koning CE, *Adv Mater*, 2004; 16: 248.
71. Fan W, Zhang C, Tjiu CW, Liu T, *J Mater Res*, 2013; 28: 611.
72. Zhan Y, Lavorgna M, Buonocore G, Xia H, *J Mater Chem*, 2012; 22: 10464.
73. Wang D, Zhang X, Zha J-W, Zhao J, Dang Z-M, Hu G-H, *Polymer*, 2013; 54: 1916.
74. Bonnet P, Sireude D, Garnier B, Chauvet O, *Appl Phys Lett*, 2007; 91: 1910.
75. Kumar SA, Alam MA, Murthy JY, *Appl Phys Lett*, 2007; 90: 104105.
76. Kirkpatrick S, *Rev Mod Phys*, 1973; 45: 574
77. Smith RJ, Lotya M, Coleman JN, *New J Phys*, 2010; 12: 125008.
78. Shahil KMF, Balandin AA, *Nano Lett*, 2012; 12: 861.
79. Juhué D, Lang J, *Colloids Surf A*, 1994; 87: 177.
80. Juhué D, Lang J, *Langmuir*, 1993; 9: 792.
81. Zuberi M, Sherman DM, Cho Y, *J Phys Chem C*, 2011; 115: 3881.
82. Lisunova MO, Lebovka NI, Melezhyk OV, Boiko YP, *J Colloid Interface Sci*, 2006; 299: 740.
83. Mohamed A, Anas AK, Abu Bakar S, Ardyani T, Zin WMW, Ibrahim S, Sagisaka M, Brown P, Eastoe J, *J Colloid Interface Sci*, 2015; 455: 179.
84. Mohamed A, Anas AK, Abu Bakar S, Aziz AA, Sagisaka M, Brown P, Eastoe J, Kamari A, Hashim N, Isa IM, *Colloid Polym Sci*, 2014; 292: 3013.
85. Potts JR, Dreyer DR, Bielawski CW, Ruoff RS, *Polymer*, 2011; 52: 5.
86. Hernández M, Bernal MDM, Verdejo R, Ezquerro TA, López-Manchado MA, *Compos Sci Technol*, 2012; 73: 40.

87. Goodwin J, Colloids and Interfaces with Surfactants and Polymers: Second edition, John Wiley & Sons, West Sussex, 2009.
88. Pitt AR, Morley SD, Burbidge NJ, Quickenden, Colloids Surf A, 1996; 114: 321.
89. Mohamed A, Trickett K, Chin SY, Cummings S, Sagisaka M, Hudson L, Nave S, Dyer R, Rogers SE, Heenan RK, Eastoe J, Langmuir, 2010; 26: 13861.
90. Shih C-J, Lin S, Strano MS, Blankschtein D, J Am Chem Soc, 2010. 132: 14638.
91. Texter J, Curr Opin Colloid Interface Sci, 2014; 19: 163.
92. Islam MF, Rojas E, Bergey DM, Johnson AT, Yodh AG, Nano Lett, 2003; 3: 269.
93. Strano MS, Moore VC, Miller MK, Allen MJ, Haroz EH, Kittrell C, Hauge RH, Smalley RE, J Nanosci Nanotechnol, 2003; 3: 81.
94. Matarredona O, Rhoads H, Li Z, Harwell JH, Balzano L, Resasco DE, J Phys Chem B, 2003; 107: 13357.
95. Moore VC, Strano MS, Haroz EH, Hauge RH, Smalley RE, Schmidt J, Talmon Y, Nano Lett, 2003; 3: 1379.
96. Rausch J, Zhuang R-C, Mäder E, Composites, Part A, 2010; 41: 1038.
97. Jiang L, Gao L, Sun J, J Colloid Interface Sci, 2003; 260: 89.
98. Jiang S, Gui Z, Bao C, Dai K, Wang X, Zhou K, Shi Y, Lo S, Hu Y, Chem Eng J, 2013; 226: 326.
99. Meyer EE, Rosenberg KJ, Israelachvili J, Proceedings of the National Academy of Sciences of the United States of America, 2006; 103: 15739.
100. Hsieh AG, Punckt C, Korkut S, Aksay IA, J Phys Chem B, 2013; 117: 7950.
101. Glover AJ, Adamson DH, Schniepp HC, J Phys Chem C, 2012; 116: 20080.
102. Suttipong M, Tummala NR, Kitiyanan B, Striolo A, J Phys Chem C, 2011; 115: 17286.
103. Zhang L, Zhang Z, He C, Dai L, Liu J, Wang L, ACS Nano, 2014; 8: 6663.

104. Shih C-J, Lin S, Strano MS, Blankschtein D, *J Phys Chem C*, 2015; 119: 1047.
105. Shih C-J, Lin S, Strano MS, Blankschtein D, *J Am Chem Soc*, 2011; 133: 12810.
106. Green AA, Hersam MC, *Nano Lett*, 2009; 9: 4031.
107. Bystrzejewski M, Huczko A, Lange H, Gemming T, Büchner B, Rummeli MH, *J Colloid Interface Sci*, 2010; 345: 138.
108. Manne S, Cleveland JP, Gaub HE, Stucky GD, Hansma PK, *Langmuir*, 1994; 10: 4409.
109. Paruchuri VK, Nguyen AV, Miller JD, *Colloids Surf A*, 2004; 250: 519.
110. Griffith A, Notley SM, *J Colloid Interface Sci*, 2012; 369: 210.
111. Wang Z, Liu J, Wang X, Chen H, Liu Z, Yu Q, Zeng H, Sun L *Chem Commun*, 2013; 49: 10835.
112. Kim JS, Hong S, Park DW, Shim SE, *Macromol Res*, 2010; 18: 558.
113. Kim JS, Yun JH, Kim I, Shim SE, *J Ind Eng Chem*, 2011; 17: 325.
114. Zhao CL, Dobler F, Pith T, Holl Y, Lambla M, *J Colloid Interface Sci*, 1989; 128: 437.
115. Wan Y-J, Tang L-C, Yan D, Zhao L, Li Y-B, Wu L-B, Jiang J-X, Lai G-Q, *Compos Sci Technol*, 2013; 82: 60.
116. Patrick HN, Warr GG, *Colloids Surf A*, 2000; 162: 149.
117. Patrick HN, Warr GG, Manne S, Aksay IA, *Langmuir*, 1997; 13: 4349.
118. Seo, J-WT, Green AA, Antaris AL, Hersam MC, *J Phys Chem Lett*, 2011; 2: 1004.
119. Israelachvili JN, Mitchell DJ, Ninham BW, *J Chem Soc Faraday Trans 2*, 1976; 72: 1525.
120. Myers D, *Surfaces, Interfaces, and Colloids: Second Edition*, Wiley-Vch, New York, 1999.

121. Texter J, Vasantha VA, Crombez R, Maniglia R, Slater L, Mourey T, *Macromol Rapid Commun*, 2012; 33: 69.
122. Bourlinos AB, Georgakilas V, Zboril R, Steriotis TA, Stubos AK, Trapalis C, *Solid State Commun*, 2009; 149: 2172.
123. Stankovich S, Piner RD, Chen X, Wu N, Nguyen ST, Ruoff RS, *J Mater Chem*, 2006; 16: 155.
124. Nativ-Roth E, Shvartzman-Cohen R, Bounioux C, Florent M, Zhang D, Szleifer I, Yerushalmi-Rozen R, *Macromolecules*, 2007; 40: 3676.
125. Shvartzman-Cohen R, Nativ-Roth E, Baskaran E, Levi-Kalisman Y, Szleifer I, Yerushalmi-Rozen R, *J Am Chem Soc*, 2004; 126: 14850.
126. O'Connell MJ, Boul P, Ericson LM, Huffman C, Wang Y, Haroz E, Kuper C, Tour J, Ausman KD, Smalley RE, *Chem Phys Lett*, 2001; 342: 265.
127. Shvartzman-Cohen R, Levi-Kalisman Y, Nativ-Roth E, Yerushalmi-Rozen R, *Langmuir*, 2004; 20: 6085.
128. Israelachvili JN, *Intermolecular and Surface Forces: Revised Third Edition*, Academic Press, Boston, 2011.
129. Rosen MJ, Kunjappu JT, *Surfactants and Interfacial Phenomena: Third Edition*, John Wiley & Sons, New Jersey, 2004.
130. Verwey EJW, Overbeek JThG, *Theory of the Stability of Lyophobic Colloids*, Elsevier Publishing Company, New York, 1948.
131. Fennel Evans D, Wennerstrom H, *The Colloidal Domain: Where Physics, Chemistry, Biology and Technology Meet*, Wiley-VCH Weinheim, New York, 1994.
132. Sun Z, Nicolosi V, Rickard D, Bergin SD, Aherne D, Coleman JN, *J Phys Chem C*, 2008; 112: 10692.

133. Tadros T. In Tadros T (editor), *Colloid Stability: The Role of Surface Forces - Part 1*, Vol. 1. Wiley-VCH Verlag GmbH & Co. KGaA; 2007. Chapter 1, pp. 1-22.
134. Rajter RF, French RH, Ching WY, Carter WC, Chiang YM, *J Apply Phys*, 2007; 101: 054303.
135. McAllister MJ, Li J-L, Adamson DH, Schniepp HC, Abdala AA, Liu J, Herrera-Alonso M, Millius DL, Car R, Prud'homme RK, *Chem Mater*, 2007; 19: 4396.
136. Blanch AJ, Lenehan CE, Quinton JS, *J Phys Chem B*, 2010; 114: 9805.
137. An X, Simmons T, Shah R, Wolfe C, Lewis KM, Washington M, Nayak SK, Talapatra S, Kar S, *Nano Lett*, 2010; 10: 4295.
138. Srinivas G, Nielsen SO, Moore PB, Klein ML, *J Am Chem Soc*, 2006; 128: 848.
139. Grant LM, Tiberg F, Ducker WA, *J Phys Chem B*, 1998; 102: 4288.
140. Holland NB, Ruegsegger M, Marchant RE, *Langmuir*, 1998; 14: 2790.
141. Yin S, Wang C, Qiu X, Xu B, Bai C, *Surf Interface Anal*, 2001; 32: 248.
142. Rabe JP, Buchholz S, *Science*, 1991; 253: 424.
143. Klevens HB, *J Am Oil Chem Soc*, 1953; 30: 74.
144. Lin D, Xing B, *Environ Sci Technol*, 2008; 42: 7254.
145. Kabe R, Feng X, Adachi C, Müllen K, *Chemistry-An Asian Journal*, 2014; 9: 3125.
146. Gotovac S, Honda H, Hattori Y, Takahashi K, Kanoh H, Kaneko K, *Nano Lett*, 2007; 7: 583.
147. Florio GM, Werblowsky TL, Müller T, Berne BJ, Flynn GW, *J Phys Chem B*, 2005; 109: 4520.
148. O'Dea AR, Smart RSC, Gerson AR, *Carbon*, 1999; 37: 1133.
149. Jiang D-e, Sumpter BG, Dai S, *J Phys Chem B*, 2006; 110: 23628.
150. Wang J, Chen Z, Chen B, *Environ Sci Technol*, 2014; 48: 4817.

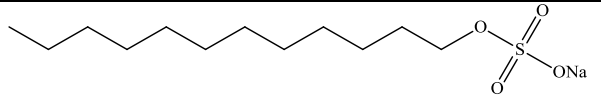
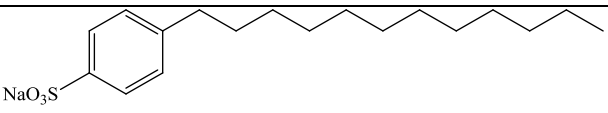
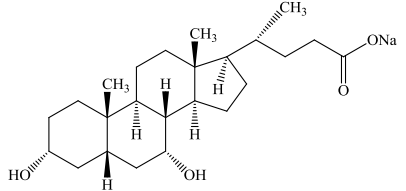
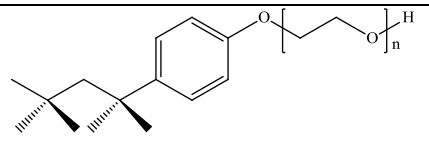
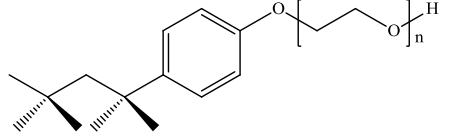
151. Björk J, Hanke F, Palma C-A, Samori P, Cecchini M, Persson M, *J Phys Chem Lett*, 2010; 1: 3407.
152. Martinez CR, Iverson BL, *Chem Sci*, 2012; 3: 2191.
153. Grimme S, *Angew Chem Int Ed*, 2008; 47: 3430.
154. Galbraith JW, Giles CH, Halliday AG, Hassan ASA, McAllister DC, Macaulay N, Macmillan NW, *J Appl Chem*, 1958; 8: 416.
155. Kim BS, Hayes RA, Ralston J, *Carbon*, 1995; 33: 25.
156. Cristadoro A, Ai M, Räder HJ, Rabe JP, Müllen K, *J Phys Chem C*, 2008; 112: 5563.
157. Radovic LR, Bockrath B, *J Am Chem Soc*, 2005; 127: 5917.
158. Subrahmanyam KS, Ghosh A, Gomathi A, Govindaraj A, Rao CNR, *Nanosci Nanotechnol Lett*, 2009; 1: 28.
159. Reczek JL, Iverson BL, *Macromolecules*, 2006; 39: 5601.
160. Andrews LJ, *Chem Rev*, 1954; 54: 713.
161. Reczek JL, Villazor KR, Lynch V, Swager TM, Iverson BL, *J Am Chem Soc*, 2006; 128: 7995.
162. Hunter CA, Sanders JKM, *J Am Chem Soc*, 1990; 112: 5525.
163. Waters ML, *Curr Opin Chem Biol*, 2002; 6: 736.
164. Nave S, Paul A, Eastoe J, Pitt AR, Heenan RK, *Langmuir*, 2005; 21: 10021.
165. Glanzer S, Sax AF, *Mol Phys*, 2013; 111: 2427.
166. Domínguez H, *J Phys Chem B*, 2007; 111: 4054.
167. Tummala NR, Grady BP, Striolo A, *Phys Chem Chem Phys*, 2010; 12: 13137.
168. Sun H, Yang X, *Colloids Surf A*, 2014; 462: 82.
169. Wu D, Yang X, *J Phys Chem B*, 2012; 116: 12048.
170. Syurik YV, Ghsilandi MG, Tkalya EE, Paterson G, McGrouther D, Ageev OA, Loos J, *Macromol Chem Phys*, 2012; 213: 1251.

171. Wu T-M, Chen E-C, *Compos Sci Technol*, 2008; 68: 2254.
172. Grossiord N, Loos J, Regev O, Koning CE, *Chem Mater*, 2006; 18: 1089.
173. Grossiord N, Loos J, van Laake L, Maugey M, Zakri C, Koning CE, Hart AJ, *Adv Funct Mater*, 2008; 18: p. 3226.
174. Syurik J, Alyabyeva N, Alekseev A, Ageev OA, *Compos Sci Technol*, 2014; 95: 38.
175. Alekseev A, Chen D, Tkalya EE, Ghislandi MG, Syurik Y, Ageev O, Loos J, de With G, *Adv Funct Mater*, 2012; 22: 1311.
176. Grossiord N, PhD Thesis, Technische Universiteit Eindhoven, 2007, Available from: <http://repository.tue.nl/632828>.
177. Rippel MM, Lee L-T, Leite CAP, Galembeck F, *J Colloid Interface Sci*, 2003; 268: 330.
178. Nawamawat K, Sakdapipanich JT, Ho CH, Ma Y, Song J, Vancso JG, *Colloids Surf A*, 2011; 390: 157.
179. Puskas JE, Chiang K, Barkakaty J. In Kohjiya S, Ikeda Y (editors), *Chemistry, Manufacture and Applications of Natural Rubber*, Woodhead Publishing; 2014. Chapter 2, pp. 30-67.
180. Hudgin DE, Bendler T, *Handbook of Polycarbonate Science and Technology*, Marcel Dekker, New York , 2000.
181. Dreyer DR, Murali S, Zhu Y, Ruoff RS, Bielawski CW, *J Mater Chem*, 2011; 21: 3443.
182. Park S, An J, Potts JR, Velamakanni A, Murali S, Ruoff RS, 2011; 49: 3019.
183. Park S, Ruoff RS, *Nat Nanotechnol*, 2009; 4: 217.
184. McCoy TM, Brown P, Eastoe J, Tabor RF, *ACS Appl Mater Interfaces*, 2015; 7: 2124.
185. Ager D, Arjunan VV, Crombez R, Texter J, *ACS Nano*, 2014; 8: 11191.

186. Liu N, Luo F, Wu H, Liu Y, Zhang C, Chen J, Adv Funct Mater, 2008; 18: 1518.

ACCEPTED MANUSCRIPT

Table 1. Surfactants featured in this study

Label	Name	Type	Structure
1	Sodium dodecylsulfate (SDS)	Anionic	
2	Sodium dodecylbenzenesulfonate (SDBS)	Anionic	
3	Sodium cholate (SC)	Anionic	
4	Cetyltrimethylammonium bromide (CTAB)	Cationic	
5	Triton-X100	Nonionic	

6	Pluronic F 127	Nonionic	<p style="text-align: right;">a = 100 b = 65</p>
7	Poly(sodium-4-styrene sulfonate) (PSS)	Polymeric	
8	Amphiphilic block copolymer	Polymeric	
9	Tween 20	Nonionic	<p style="text-align: center;">w+x+y+z=20</p>
10	Tween 80	Nonionic	<p style="text-align: center;">w+x+y+z=20</p>
11	IGEPAL CO-890	Nonionic	<p style="text-align: center;">n = 40</p>

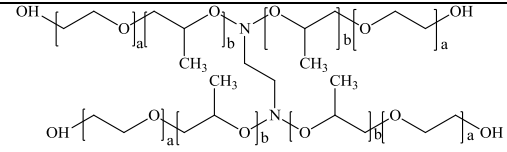
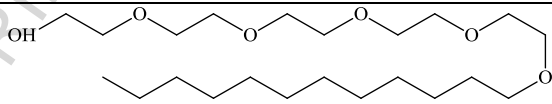
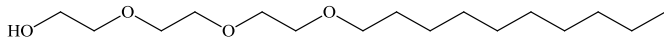
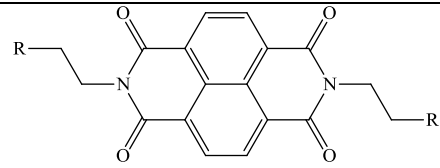
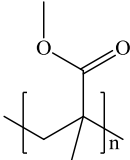
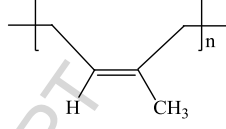
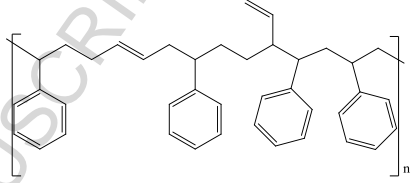
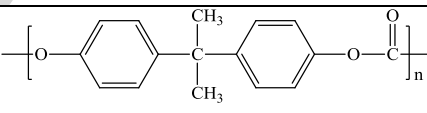
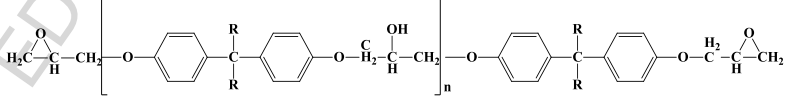
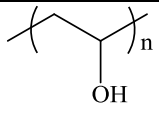
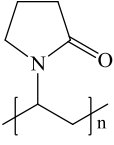
12	Tetronic	Nonionic	
13	Penta(oxyethylene)- <i>n</i> -dodecyl ether (C12E5)	Nonionic	
14	Tri(oxyethylene)- <i>n</i> -decyl ether (C10E3)	Nonionic	
15	Napthalene diimide (NDI)	Ionic	 <p> R = COONa (NDI-1) R = SO₃Na (NDI-2) </p>

Table 2. Polymers featured in this review

Label	Polymer name	Structure
1	Poly(methyl methacrylate) (PMMA)	 The image shows the chemical structure of the repeating unit of Poly(methyl methacrylate) (PMMA). It consists of a carbon-carbon backbone where each carbon is bonded to a hydrogen atom and a methyl group. The second carbon is also bonded to a methoxy carbonyl group (-COOCH ₃). The entire unit is enclosed in brackets with a subscript 'n'.

2	Natural Rubber (NR)	
3	Styrene Butadiene Rubber (SBR)	
4	Polycarbonate (PC)	
5	Epoxy Resin	 <p> R = CH₃ (Bisphenol A) R = H (Bisphenol F) </p>
6	Poly(vinyl alcohol) (PVA)	
7	Polyvinyl pyrrolidone (PVP)	

8	PP (Polypropylene)	 <p>The diagram shows the repeating unit of polypropylene (PP) enclosed in large square brackets with a subscript 'n'. The unit consists of a carbon-carbon backbone. The left carbon is bonded to a hydrogen atom (H) pointing downwards. The right carbon is bonded to a methyl group (CH₃) pointing upwards and a hydrogen atom (H) pointing downwards. The bonds extending from the carbons to the left and right of the brackets represent the polymer chain continuation.</p>
9	Polystyrene (PS)	 <p>The diagram shows the repeating unit of polystyrene (PS) enclosed in large square brackets with a subscript 'n'. The unit consists of a carbon-carbon backbone. The left carbon is bonded to a hydrogen atom (H) pointing downwards. The right carbon is bonded to a hydrogen atom (H) pointing downwards and a phenyl ring (a benzene ring) pointing upwards. The bonds extending from the carbons to the left and right of the brackets represent the polymer chain continuation.</p>

Table 3. Graphene dispersions stabilized by different surfactants

Surfactant	cmc ^a	Preparation method	Stability	C _{surf} ^b	C _{Gi} ^c (mg mL ⁻¹)	C _{Gf} ^d (mg mL ⁻¹)	Cost ^e (US\$ g ⁻¹)	Reference
SDS	2.50 mg mL ⁻¹	Liquid-phase exfoliation (tip ultrasonication; 30 min)	(7 days) ^f	0.1 ^g	5.0	0.011	0.75	77
SDBS	0.70 – 0.73 mg mL ⁻¹	Liquid-phase exfoliation (bath ultrasonication; 30 min)	~6 weeks	0.5 – 10.0 ^g	0.1 – 10.0	0.002 – 0.050	0.10	60
		Liquid-phase exfoliation (tip ultrasonication; 30 min)	(7 days) ^f	0.1 ^g	5.0	~0.020		77
SC	5.00 mg mL ⁻¹	Liquid-phase exfoliation (bath ultrasonication; up to 430 h)	(5 days) ^f	0.1 ^g	5.0	0.300	1.20	57
		Liquid-phase exfoliation (horn ultrasonication; 1 h)	Several weeks	2.0 ^h	85.7	0.090		106
		Liquid-phase exfoliation (tip ultrasonication; 30 min)	(7 days) ^f	0.1 ^g	5.0	0.026		77

		ultrasonication 30 min)						
CTAB	0.36 mg mL ⁻¹ ; 1.00 mM	Liquid-phase exfoliation (ultrasonication; 5 min)	>6 months	0.1 – 0.9 ⁱ	1.0 ^h	~0.550	1.25	110
		Liquid-phase exfoliation (ultrasonication 12h)	>15 days	3.3 – 25.0 ^g	1.7	-		111
		Liquid-phase exfoliation (tip ultrasonication; 30 min)	(7 days) ^f	0.1 ^g	5.0	~0.019		77
Triton-X100	0.34 mg mL ⁻¹	Liquid-phase exfoliation (tip ultrasonication; 30 min)	(7 days) ^f	0.1 ^g	5.0	~0.021	0.40	77
Pluronic F 127	-	Liquid-phase exfoliation (horn ultrasonication; 30 min)	-	1.0 ^h	75.0	0.064	0.18	118
PSS	-	Reduction of GO in the presence of surfactant	>1 year	10.0 ^g	1.0	1.0	0.50	123
Tween 20	0.02 mg mL ⁻¹	Liquid-phase exfoliation (tip ultrasonication; 30 min)	(7 days) ^f	0.1 ^g	5.0	~0.022	0.07	77
Tween 80	0.07 mg mL ⁻¹	Liquid-phase exfoliation (tip ultrasonication; 30 min)	(7 days) ^f	0.1 ^g	5.0	~0.020	0.08	77
IGEPAL CO-890	0.59 mg mL ⁻¹	Liquid-phase exfoliation (tip ultrasonication; 30 min)	(7 days) ^f	0.1 ^g	5.0	0.026	0.51	77

Tetronic	-	Liquid-phase exfoliation (horn ultrasonication; 30 min)	-	1.0 ^h	75.0	0.038 – 0.086	0.18	118
NDI	-	Liquid phase exfoliation (horn ultrasonication; 1 h)	4 months	1.0 – 10.0 ^g	100.0	1.200 – 5.000	32.0 – 60.0	103

^aCritical micelle concentration. ^bSurfactant concentration. ^cInitial graphite concentration. ^dFinal graphene concentration. ^eBased on precursor of custom made surfactant or commercial surfactant prices at current rates from scientific suppliers. ^fValues in parentheses are the time required to re-measuring the stability after sample preparation. ^gmg mL⁻¹. ^hwt%. ⁱmM.

Table 4. Graphene/polymer nanocomposite electrical properties

Polymer	Surfactant		Filler		Percolation threshold	Conductivity (σ ; S cm ⁻¹)		Reference
	Name	Amount	Type	Loading		Matrix	Composite	
PMMA	SDS	59.4 ^b	FGN	1.0 – 4.0 ^d	-	-	-	98
NR	SDS	1 : 3 ^c	TRGO	1.0 – 4.0 ^e	-	$\sim 10^{-12}$	10^{-6}	61
	Pluronic F-127	1 : 3 ^c	TRGO	1.0 – 4.0 ^e	-	$\sim 10^{-12}$	10^{-9}	61
	CTAB	13.7 ^b ; 0.5 ^d	rGO	0.01 – 10.0 ^d	0.1 – 0.5 ^d	$\sim 10^{-7}$	10^{-3}	44
SBR	CTAB	0.9 ^b	MLG	0.0 – 5.0 ^d	0.5 – 1.0 ^d	4.52×10^{-13}	4.56×10^{-7}	113
	CTAB	0.9 ^b	MLG	0.0 – 5.0 ^d	$\sim 0.5^d$	$\sim 10^{-13}$	8.24×10^{-6}	112
PC	Triton-X100	-	Graphene nanosheet	0.027 – 2.2 ^f	0.14 ^f	2.05×10^{-13}	0.512	42
Epoxy Resin	SC	46.45 ^b ; 2.0 ^d	Graphene-MLG	1.0 – 10.0 ^f	-	-	1.4×10^{-9}	78
	Triton-X100	$\sim 2.32^b$	TRGO	0.0 – 0.2 ^d	-	-	-	115
PVA	Amphiphilic block copolymer	3 : 1 ^c	Graphene	1.0 – 5.0 ^d	-	$\sim 10^{-12}$	$\sim 10^{-13}$	62

PP	SDBS	1 : 2 ^c	Graphene	0.1 – 10.0 ^d	1.2 – 1.5 ^d	-	9.2 x 10 ⁻³	38
	PSS	1 : 10 ^g	rGO	0.0 – 2.0 ^d	0.4 ^d	10 ⁻⁹	4 x 10 ⁻³	170
PS	SC	1 : 1 ^c	Exfoliated TRGO + Liquid phase exfoliation graphite ^h	0.5 – 12.0 ^d	2.0 – 4.5 ^d	-	~0.1	28
	PSS	1 : 10 ^g	rGO	0.0 – 2.0 ^d	0.9 ^d	10 ⁻¹¹	0.12	170
	PSS	1 : 10 ^g	rGO	0.0 – 2.0 ^d	0.8 – 0.9 ^d	10 ⁻¹¹	~0.15	27
	PSS	1 : 10 ^g	rGO	1.9 ^d	-	-	-	175
	PSS	1 : 10 ^g	GNP	0.0 – 2.0 ^d	~0.9 ^d	10 ⁻¹¹	~0.12	174

^aFGN: functionalized graphene; TRGO: thermally reduced graphene oxide; rGO: reduced graphene oxide (chemical reduction); MLG: multilayer graphene; GNP: graphene nanoplatelet.

^bConcentration in mM. ^cRatio of nanofiller to surfactant. ^dwt%. ^ephr. ^fvol%. ^gRatio of graphene oxide to the amount of surfactant used during chemical reduction of graphene oxide. ^hThe graphene dispersions were prepared with four different methods.

Table 5. Enhancement of properties and applications of graphene/polymer nanocomposites

Polymer	Surfactant used	Filler		Property enhancement	Potential application	Reference
		Type ^a	Loading			
PMMA	SDS	FGN	1.0 – 4.0 ^b	Glass transition temperature (T _g) Tensile strength Storage modulus	-	98
NR	SDS	TRGO	1.0 – 4.0 ^c	Electrical conductivity Elastic modulus Maximum strength	-	61

	Pluronic F-127	TRGO	1.0 – 4.0 ^c	Electrical conductivity Elastic modulus Maximum strength	-	61
	CTAB	rGO	0.01 – 10.0 ^b	Storage modulus Solvent/chemical resistance Microorganism resistance Electrical conductivity	Acoustic insulation Food packaging Hygiene product, biomedic	44
SBR	CTAB	MLGS	0.0 – 5.0 ^b	Electrical conductivity Thermal stability	-	113
	CTAB	MLGS	0.0 – 5.0 ^b	Electrical conductivity	-	112

				Thermal stability		
PC	Triton-X100	Graphene nanosheet	0.027 – 2.2 ^d	Electrical conductivity Storage modulus	Air vehicle component	42
Epoxy Resin	SC	Graphene-MLG	1.0 – 10.0 ^d	Thermal conductivity	Thermal interface materials	78
	Triton-X100	TRGO	0.0 – 0.2 ^b	Thermal stability Tensile strength	-	115
PVA	Amphiphilic block copolymer	Graphene	1.0 – 5.0 ^b	Thermal stability	-	62
PP	SDBS	Graphene	0.1 – 10.0 ^b	Electrical conductivity	-	38
	PSS	rGO	0.0 – 2.0 ^b	Electrical conductivity	Antistatic and electromagnetic interference shielding	170
PS	SC	Exfoliated TRGO + Liquid phase exfoliation	0.5 – 12.0 ^b	Electrical conductivity	-	28

		graphite ^g				
	PSS	rGO	0.0 – 2.0 ^b	Electrical conductivity	Antistatic and electromagnetic interference shielding	170
	PSS	rGO	0.0 – 2.0 ^b	Electrical conductivity	-	27
	PSS	rGO	1.9 ^b	-	-	175
	PSS	GNP	0.0 – 2.0 ^b	Electrical conductivity	-	174

^aFGN: functionalized graphene; TRGO: thermally reduced graphene oxide; rGO: reduced graphene oxide (chemical reduction); MLG: multilayer graphene; GNP: graphene nanoplatelet. ^bwt%. ^cphr. ^dvol%.

List of Figures

Fig.1. Schematic diagram of graphene/polymer nanocomposite preparation using latex technology. Reprinted with permission from Ref. [27].

Fig.2. SEM images of MWCNTs and graphene organized respectively: (a and d) as powder compacts, (b and e) as paper films and (c and f) inside PP polymer composites. It is possible to see partially wrapped graphene platelets inside the PP polymer matrix (f). Reprinted with permission from Ref. [38].

Fig.3. Variation of zeta potential with pH for (a) SBR latex, (b) MLGS-COOH in water, and (c) MLGS+CTAB in water. Reprinted with permission from Ref. [112].

Fig.4. (A) Zeta potentials for a fresh graphene–SDBS dispersion ($C_{\text{SDBS}} = 0.5$ mg/ml, $C_{\text{G}} = 0.006$ mg/ml), and SDBS dispersion ($C_{\text{SDBS}} = 0.5$ mg/ml), and aged (6 week old) graphene–SDBS dispersion ($C_{\text{SDBS}} = 0.5$ mg/ml, $C_{\text{G}} = 0.002$ mg/ml). NB, the aged sample had a reduced C_{G} due

to sedimentation over the course of 6 weeks. Inset: Zeta potential as a function of pH for SDBS–graphene dispersions ($C_{\text{SDBS}} = 0.5$ mg/ml, $C_{\text{G}} = 0.005$ mg/ml). The natural pH of the as-prepared graphene–SDBS dispersion was 7.4, and pH was varied by addition of HCl or NaOH solutions. (B) Absorbance ($\lambda = 650$ nm) as a function of time for a $C_{\text{G}} = 0.006$ mg/ml, $C_{\text{SDBS}} = 0.5$ mg/mL sample. The curve has been fitted to a double exponential decay with the fit constants shown in the annotation. (C) Plot of the total interaction potential per unit area for two charged parallel sheets separated by distance D . The DLVO and vdW components are also shown for comparison. This graph was calculated using eq 1 and taking $\epsilon_r = 80$, $\kappa^{-1} = 8.1$ nm, $\zeta = 50$ mV, and $\rho^2 C = 6.69 \times 10^{-40}$ J m². Inset: Graph of upper and lower limits of $V_{T, \text{Max}}$, as a function of zeta potential. Reprinted with permission from Ref. [60]. Copyright (2009) American Chemical Society.

Fig.5. Plausible adsorbed states of phenanthrene and tetracene molecules on the basal plane of graphite (a) and on (n,m = 13,9) chiral SWCNT (b) surfaces (red, phenanthrene; yellow, tetracene; green, pentacene). Hydrogen atoms are omitted for clarity. Reprinted with permission from Ref. [146]. Copyright (2007) American Chemical Society.

Fig.6. Side and front views of representative simulation snapshots for the self-assembly of SDBS surfactants absorbed on graphene sheets: (a) at low surface coverage; (b) at high surface coverage. Colour code: green for CH_n groups; purple for carbon atoms in benzene rings; yellow for

sulfur atoms; red for oxygen atoms; blue for sodium counterions; orange for carbon atoms in graphene; the hydrogen atoms in benzene rings and water molecules are not shown for clarity. Reprinted with permission from Ref. [168].

Fig.7. Two possible models for the structure of the rubber latex particle surface. (A) A current model of an NR latex particle surrounded by a double-layer of proteins and phospholipids, and (B) the proposed new model consisting of a mixed layer of proteins and phospholipids around the latex particle. Reprinted with permission from Ref. [178].

Fig.1.

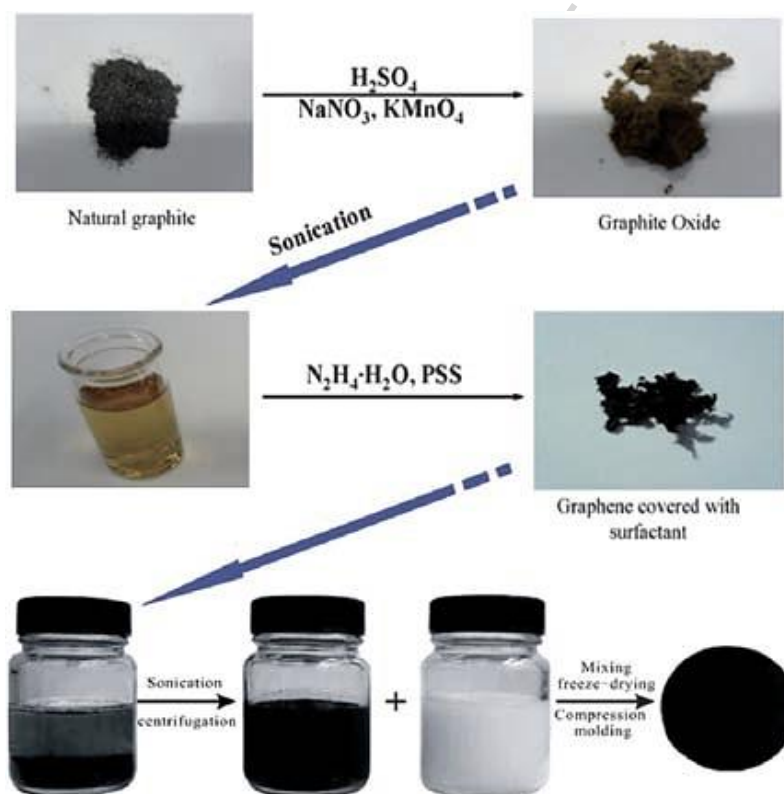


Fig.2.

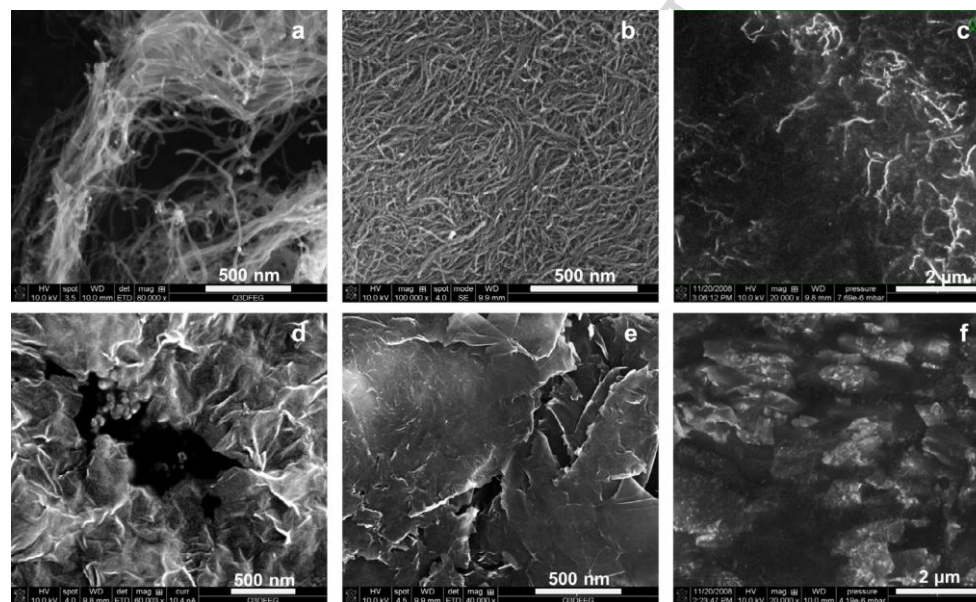


Fig.3.

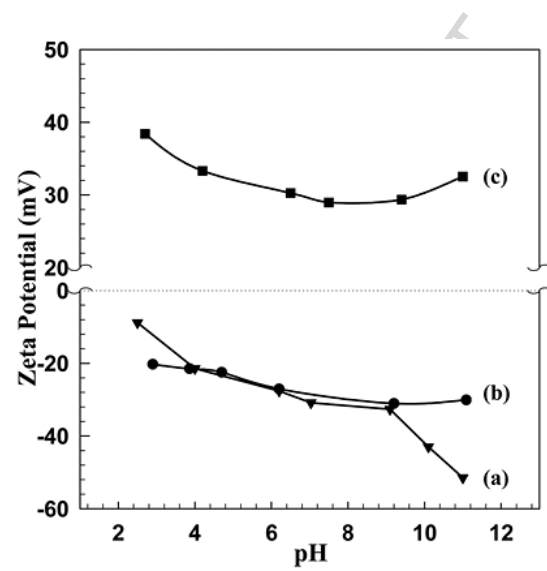


Fig.4.

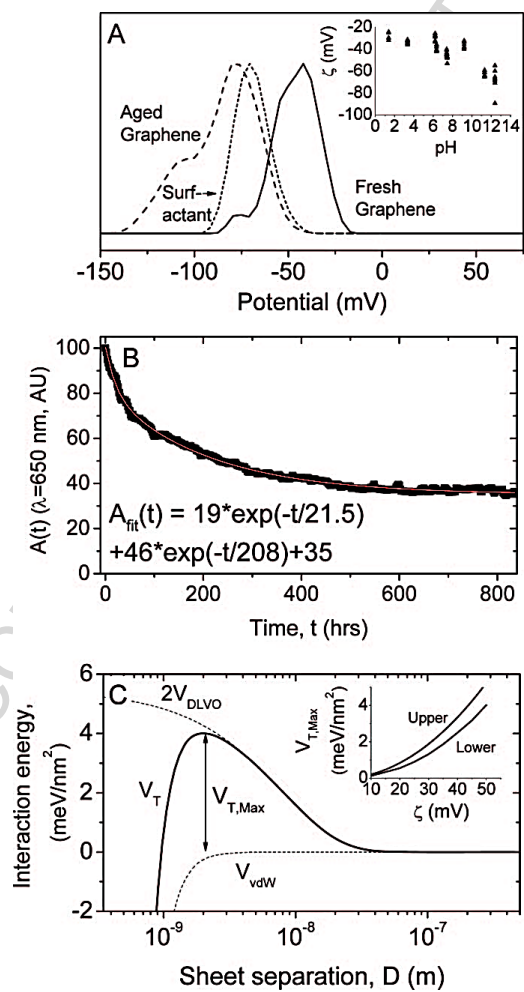


Fig.5.

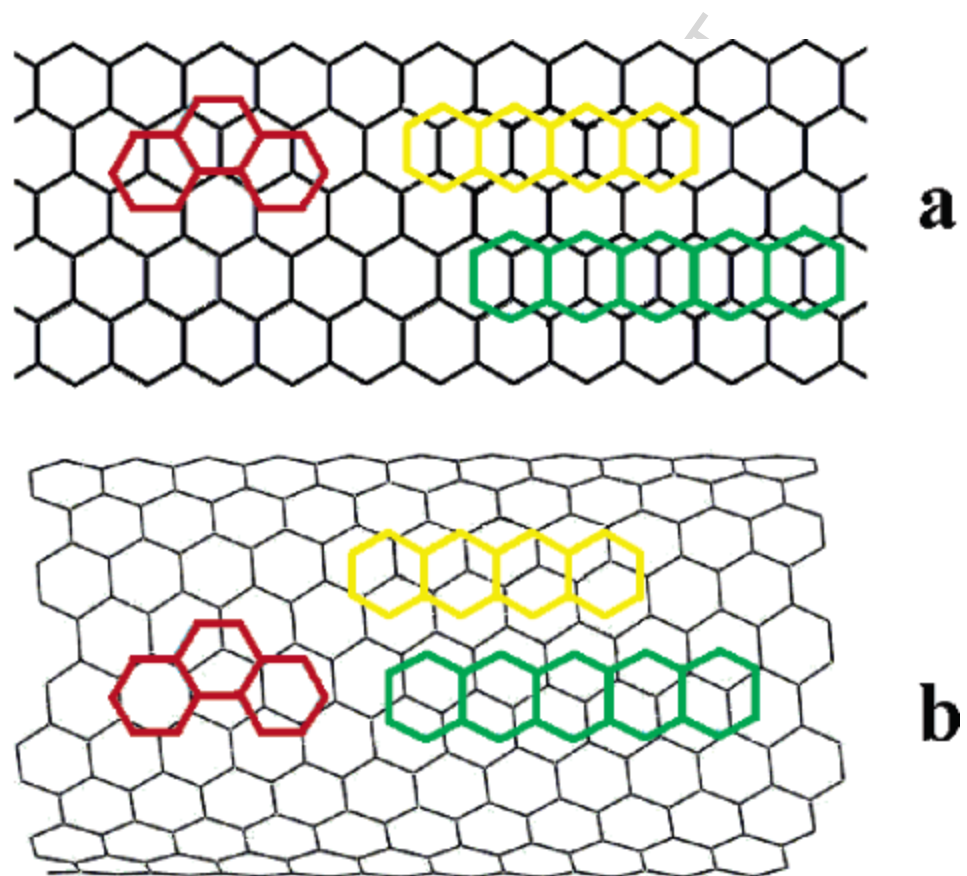


Fig.6.

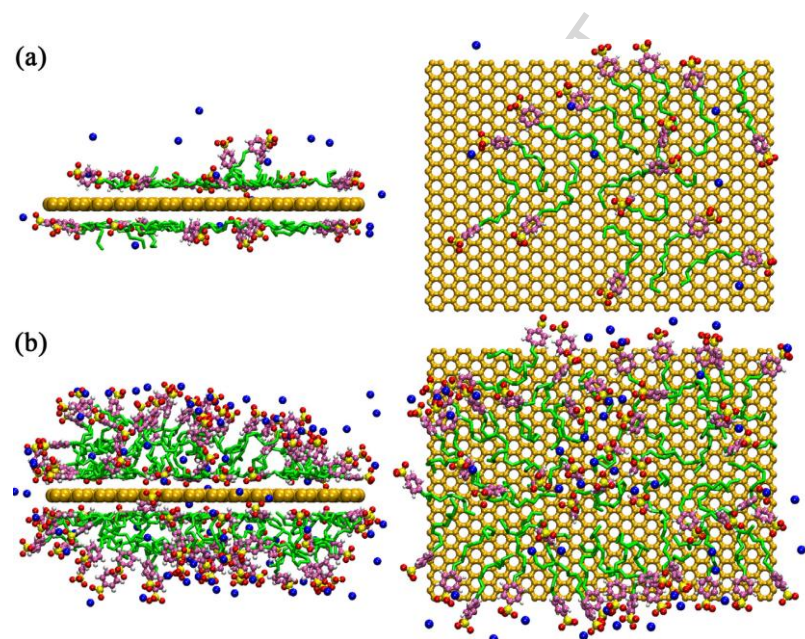
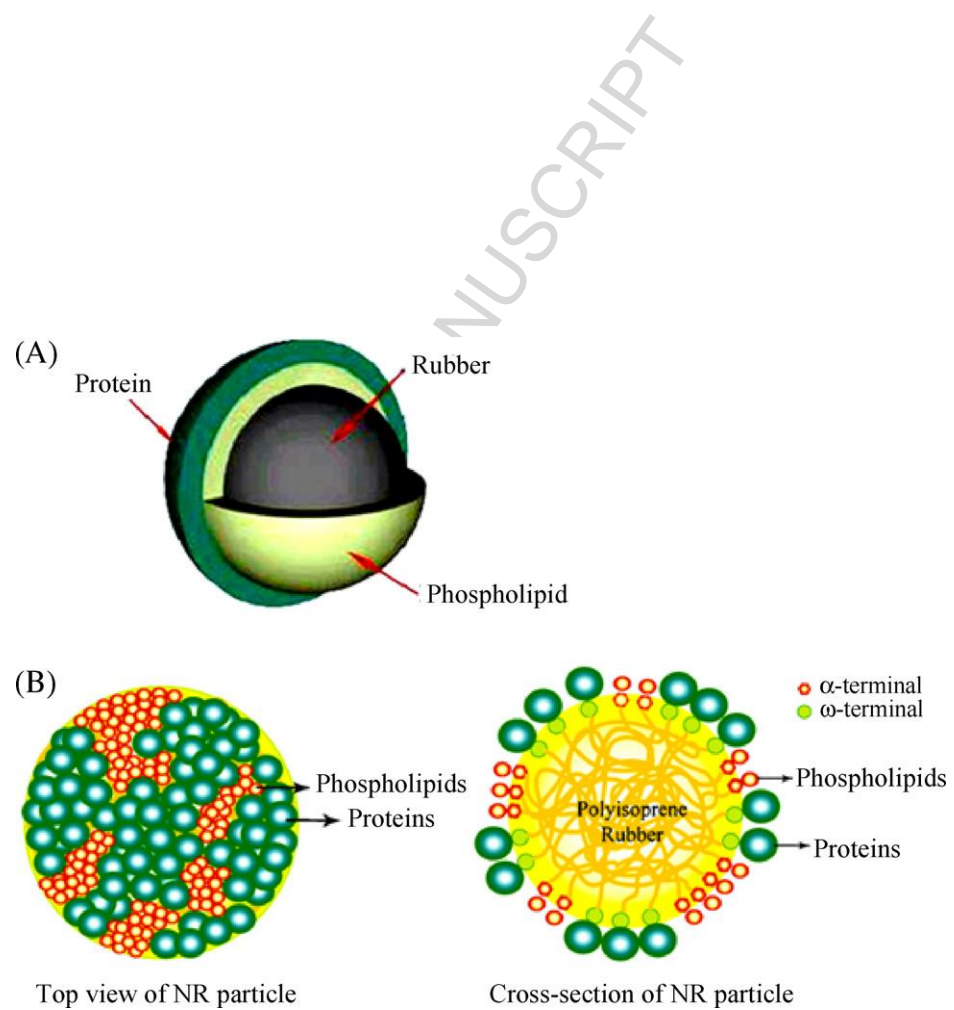
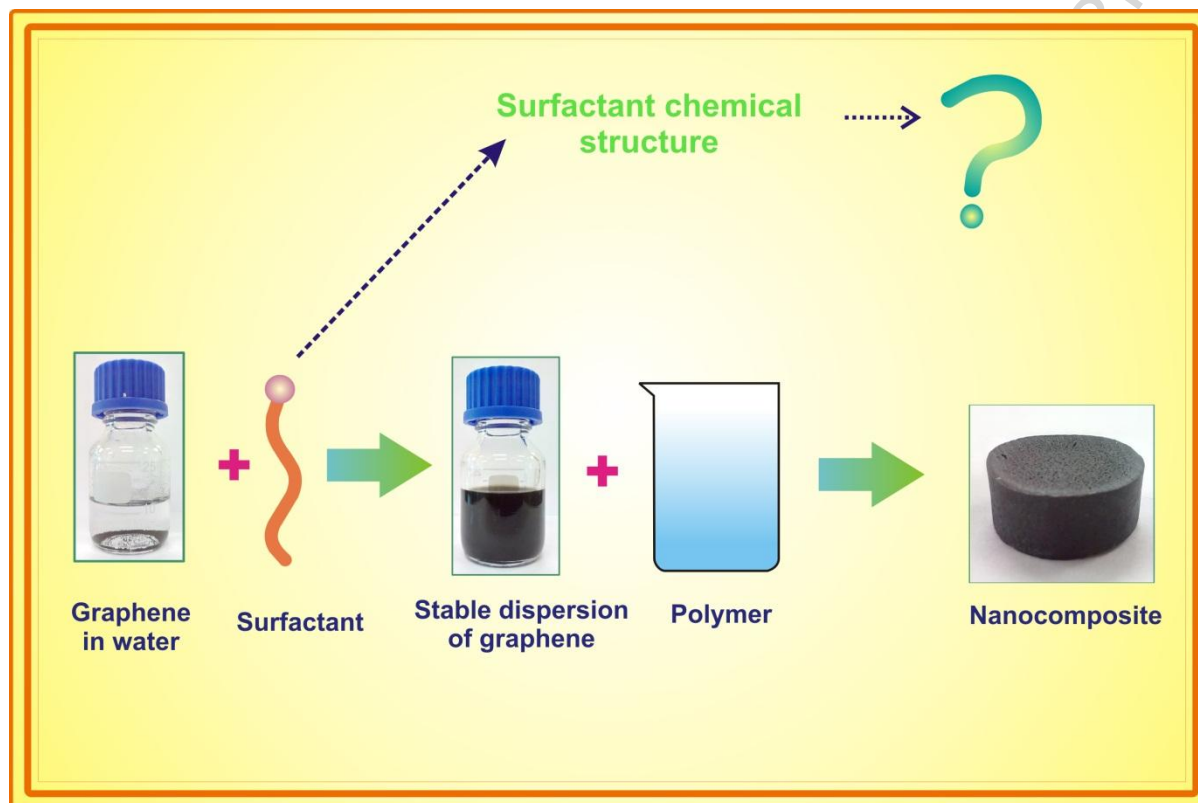


Fig.7.



Graphical Abstract



Research Highlights

- Review of current graphene-compatible surfactants for latex technology
- Surfactant chemical structure is important to achieve graphene-compatibility
- Mechanism of stabilization by surfactants
- Polymers used for latex technology

ACCEPTED MANUSCRIPT